

Materials for electrochemical capacitors

Electrochemical capacitors, also called supercapacitors, store energy using either ion adsorption (electrochemical double layer capacitors) or fast surface redox reactions (pseudo-capacitors). They can complement or replace batteries in electrical energy storage and harvesting applications, when high power delivery or uptake is needed. A notable improvement in performance has been achieved through recent advances in understanding charge storage mechanisms and the development of advanced nanostructured materials. The discovery that ion desolvation occurs in pores smaller than the solvated ions has led to higher capacitance for electrochemical double layer capacitors using carbon electrodes with subnanometre pores, and opened the door to designing high-energy density devices using a variety of electrolytes. Combination of pseudo-capacitive nanomaterials, including oxides, nitrides and polymers, with the latest generation of nanostructured lithium electrodes has brought the energy density of electrochemical capacitors closer to that of batteries. The use of carbon nanotubes has further advanced micro-electrochemical capacitors, enabling flexible and adaptable devices to be made. Mathematical modelling and simulation will be the key to success in designing tomorrow's high-energy and high-power devices.

PATRICE SIMON^{1,2} AND YURY GOGOTSI³

¹Université Paul Sabatier, CIRIMAT, UMR-CNRS 5085, 31062 Toulouse Cedex 4, France

²Institut Universitaire de France, 103 Boulevard Saint Michel, 75005 Paris, France

³Department of Materials Science & Engineering, Drexel University, 3141 Chestnut Street, Philadelphia 19104, USA

e-mail: simon@chimie.ups-tlse.fr; gogotsi@drexel.edu

Climate change and the decreasing availability of fossil fuels require society to move towards sustainable and renewable resources. As a result, we are observing an increase in renewable energy production from sun and wind, as well as the development of electric vehicles or hybrid electric vehicles with low CO₂ emissions. Because the sun does not shine during the night, wind does not blow on demand and we all expect to drive our car with at least a few hours of autonomy, energy storage systems are starting to play a larger part in our lives. At the forefront of these are electrical energy storage systems, such as batteries and electrochemical capacitors (ECs)¹. However, we need to improve their performance substantially to meet the higher requirements of future systems, ranging from portable electronics to hybrid electric vehicles and large industrial equipment, by developing new materials and advancing our understanding of the electrochemical interfaces at the nanoscale. Figure 1 shows the plot of power against energy density, also called a Ragone plot², for the most important energy storage systems.

Lithium-ion batteries were introduced in 1990 by Sony, following pioneering work by Whittingham, Scrosati and Armand (see ref. 3 for a review). These batteries, although costly, are the best in terms of performance, with energy densities that can reach 180 watt hours

per kilogram. Although great efforts have gone into developing high-performance Li-ion and other advanced secondary batteries that use nanomaterials or organic redox couples⁴⁻⁶, ECs have attracted less attention until very recently. Because Li-ion batteries suffer from a somewhat slow power delivery or uptake, faster and higher-power energy storage systems are needed in a number of applications, and this role has been given to the ECs⁷. Also known as supercapacitors or ultracapacitors, ECs are power devices that can be fully charged or discharged in seconds; as a consequence, their energy density (about 5 Wh kg⁻¹) is lower than in batteries, but a much higher power delivery or uptake (10 kW kg⁻¹) can be achieved for shorter times (a few seconds)¹. They have had an important role in complementing or replacing batteries in the energy storage field, such as for uninterruptible power supplies (back-up supplies used to protect against power disruption) and load-levelling. A more recent example is the use of electrochemical double layer capacitors (EDLCs) in emergency doors (16 per plane) on an Airbus A380, thus proving that in terms of performance, safety and reliability ECs are definitely ready for large-scale implementation. A recent report by the US Department of Energy⁸ assigns equal importance to supercapacitors and batteries for future energy storage systems, and articles on supercapacitors appearing in business and popular magazines show increasing interest by the general public in this topic.

Several types of ECs can be distinguished, depending on the charge storage mechanism as well as the active materials used. EDLCs, the most common devices at present, use carbon-based active materials with high surface area (Fig. 2). A second group of ECs, known as pseudo-capacitors or redox supercapacitors, uses fast and reversible surface or near-surface reactions for charge storage. Transition metal oxides as well as electrically conducting polymers are examples of

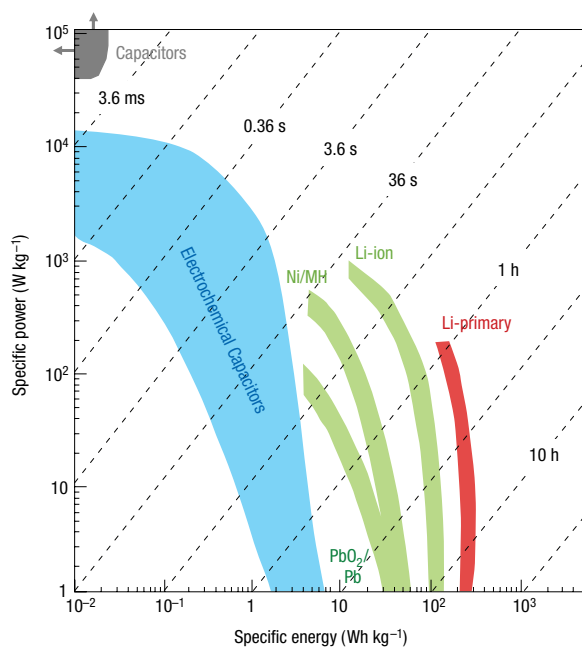


Figure 1 Specific power against specific energy, also called a Ragone plot, for various electrical energy storage devices. If a supercapacitor is used in an electric vehicle, the specific power shows how fast one can go, and the specific energy shows how far one can go on a single charge. Times shown are the time constants of the devices, obtained by dividing the energy density by the power.

pseudo-capacitive active materials. Hybrid capacitors, combining a capacitive or pseudo-capacitive electrode with a battery electrode, are the latest kind of EC, which benefit from both the capacitor and the battery properties.

Electrochemical capacitors currently fill the gap between batteries and conventional solid state and electrolytic capacitors (Fig. 1). They store hundreds or thousands of times more charge (tens to hundreds of farads per gram) than the latter, because of a much larger surface area ($1,000\text{--}2,000\text{ m}^2\text{ g}^{-1}$) available for charge storage in EDLC. However, they have a lower energy density than batteries, and this limits the optimal discharge time to less than a minute, whereas many applications clearly need more⁹. Since the early days of EC development in the late 1950s, there has not been a good strategy for increasing the energy density; only incremental performance improvements were achieved from the 1960s to 1990s. The impressive increase in performance that has been demonstrated in the past couple of years is due to the discovery of new electrode materials and improved understanding of ion behaviour in small pores, as well as the design of new hybrid systems combining faradic and capacitive electrodes. Here we give an overview of past and recent findings as well as an analysis of what the future holds for ECs.

ELECTROCHEMICAL DOUBLE-LAYER CAPACITORS

The first patent describing the concept of an electrochemical capacitor was filed in 1957 by Becker⁹, who used carbon with a high specific surface area (SSA) coated on a metallic current collector in a sulphuric acid solution. In 1971, NEC (Japan) developed aqueous-electrolyte capacitors under the energy company SOHIO's licence for power-saving units in electronics, and this application can be considered as the starting point for electrochemical capacitor use in commercial devices⁹. New applications in mobile electronics, transportation

(cars, trucks, trams, trains and buses), renewable energy production and aerospace systems¹⁰ bolstered further research.

MECHANISM OF DOUBLE-LAYER CAPACITANCE

EDLCs are electrochemical capacitors that store the charge electrostatically using reversible adsorption of ions of the electrolyte onto active materials that are electrochemically stable and have high accessible SSA. Charge separation occurs on polarization at the electrode–electrolyte interface, producing what Helmholtz described in 1853 as the double layer capacitance C :

$$C = \frac{\epsilon_r \epsilon_0 A}{d} \quad \text{or} \quad C/A = \frac{\epsilon_r \epsilon_0}{d} \quad (1)$$

where ϵ_r is the electrolyte dielectric constant, ϵ_0 is the dielectric constant of the vacuum, d is the effective thickness of the double layer (charge separation distance) and A is the electrode surface area.

This capacitance model was later refined by Gouy and Chapman, and Stern and Geary, who suggested the presence of a diffuse layer in the electrolyte due to the accumulation of ions close to the electrode surface. The double layer capacitance is between 5 and $20\ \mu\text{F cm}^{-2}$ depending on the electrolyte used¹¹. Specific capacitance achieved with aqueous alkaline or acid solutions is generally higher than in organic electrolytes¹¹, but organic electrolytes are more widely used as they can sustain a higher operation voltage (up to 2.7 V in symmetric systems). Because the energy stored is proportional to voltage squared according to

$$E = \frac{1}{2} CV^2 \quad (2)$$

a three-fold increase in voltage, V , results in about an order of magnitude increase in energy, E , stored at the same capacitance.

As a result of the electrostatic charge storage, there is no faradic (redox) reaction at EDLC electrodes. A supercapacitor electrode must be considered as a blocking electrode from an electrochemical point of view. This major difference from batteries means that there is no limitation by the electrochemical kinetics through a polarization resistance. In addition, this surface storage mechanism allows very fast energy uptake and delivery, and better power performance. The absence of faradic reactions also eliminates the swelling in the active material that batteries show during charge/discharge cycles. EDLCs can sustain millions of cycles whereas batteries survive a few thousand at best. Finally, the solvent of the electrolyte is not involved in the charge storage mechanism, unlike in Li-ion batteries where it contributes to the solid–electrolyte interphase when graphite anodes or high-potential cathodes are used. This does not limit the choice of solvents, and electrolytes with high power performances at low temperatures (down to $-40\text{ }^\circ\text{C}$) can be designed for EDLCs. However, as a consequence of the electrostatic surface charging mechanism, these devices suffer from a limited energy density. This explains why today's EDLC research is largely focused on increasing their energy performance and widening the temperature limits into the range where batteries cannot operate⁹.

HIGH SURFACE AREA ACTIVE MATERIALS

The key to reaching high capacitance by charging the double layer is in using high SSA blocking and electronically conducting electrodes. Graphitic carbon satisfies all the requirements for this application, including high conductivity, electrochemical stability and open porosity¹². Activated, templated and carbide-derived carbons¹³, carbon fabrics, fibres, nanotubes¹⁴, onions¹⁵ and nanohorns¹⁶ have been tested for EDLC applications¹¹, and some of these carbons are shown in Fig. 2a–d. Activated carbons are the most widely used materials today, because of their high SSA and moderate cost.

Activated carbons are derived from carbon-rich organic precursors by carbonization (heat treatment) in inert atmosphere

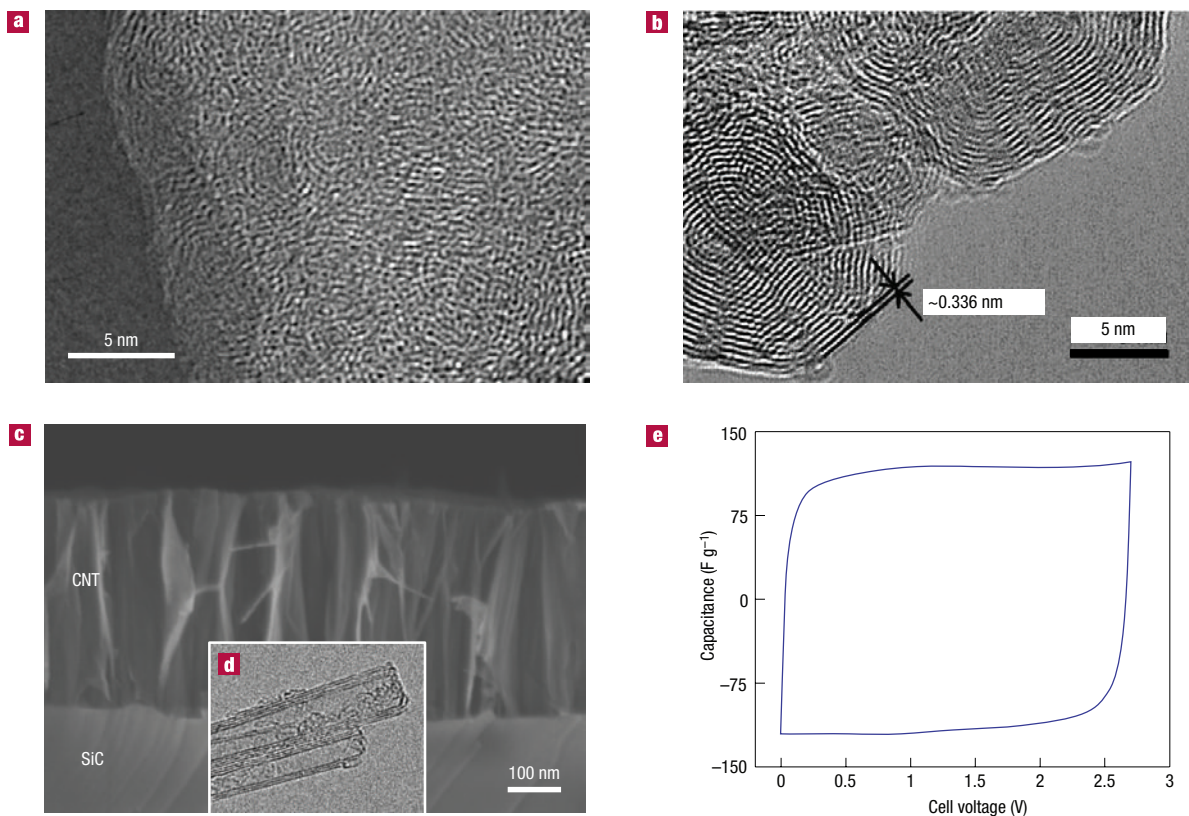


Figure 2 Carbon structures used as active materials for double layer capacitors. **a**, Typical transmission electronic microscopy (TEM) image of a disordered microporous carbon (SiC-derived carbon, 3 hours chlorination at 1,000 °C). **b**, TEM image of onion-like carbon. Reproduced with permission from ref. 80. © 2007 Elsevier. **c**, Scanning electron microscopy image of an array of carbon nanotubes (labelled CNT) on SiC produced by annealing for 6 h at 1,700 °C; inset, **d**, shows a TEM image of the same nanotubes⁷². **e**, Cyclic voltammetry of a two-electrode laboratory EDLC cell in 1.5 M tetraethylammonium tetrafluoroborate $\text{NEt}_4^+\text{BF}_4^-$ in acetonitrile-based electrolyte, containing activated carbon powders coated on aluminium current collectors. Cyclic voltammetry was recorded at room temperature and potential scan rate of 20 mV s^{-1} .

with subsequent selective oxidation in CO_2 , water vapour or KOH to increase the SSA and pore volume. Natural materials, such as coconut shells, wood, pitch or coal, or synthetic materials, such as polymers, can be used as precursors. A porous network in the bulk of the carbon particles is produced after activation; micropores (<2 nm in size), mesopores (2–50 nm) and macropores (>50 nm) can be created in carbon grains. Accordingly, the porous structure of carbon is characterized by a broad distribution of pore size. Longer activation time or higher temperature leads to larger mean pore size. The double layer capacitance of activated carbon reaches 100–120 F g^{-1} in organic electrolytes; this value can exceed 150–300 F g^{-1} in aqueous electrolytes, but at a lower cell voltage because the electrolyte voltage window is limited by water decomposition. A typical cyclic voltammogram of a two-electrode EDLC laboratory cell is presented in Fig. 2e. Its rectangular shape is characteristic of a pure double layer capacitance mechanism for charge storage according to:

$$I = C \times \frac{dV}{dt} \quad (3)$$

where I is the current, (dV/dt) is the potential scan rate and C is the double layer capacitance. Assuming a constant value for C , for a given scan rate the current I is constant, as can be seen from Fig. 2e, where the cyclic voltammogram has a rectangular shape.

As previously mentioned, many carbons have been tested for EDLC applications and a recent paper¹¹ provides an overview of

what has been achieved. Untreated carbon nanotubes¹⁷ or nanofibres have a lower capacitance (around 50–80 F g^{-1}) than activated carbon in organic electrolytes. It can be increased up to 100 F g^{-1} or greater by grafting oxygen-rich groups, but these are often detrimental to cyclability. Activated carbon fabrics can reach the same capacitance as activated carbon powders, as they have similar SSA, but the high price limits their use to speciality applications. The carbons used in EDL capacitors are generally pre-treated to remove moisture and most of the surface functional groups present on the carbon surface to improve stability during cycling, both of which can be responsible for capacitance fading during capacitor ageing as demonstrated by Azais *et al.*¹⁸ using NMR and X-ray photoelectron spectroscopy techniques. Pandolfo *et al.*¹¹, in their review article, concluded that the presence of oxygenated groups also contributes to capacitor instability, resulting in an increased series resistance and deterioration of capacitance. Figure 3 presents a schematic of a commercial EDLC, showing the positive and the negative electrodes as well as the separator in rolled design (Fig. 3a,b) and flat design (button cell in Fig. 3c).

CAPACITANCE AND PORE SIZE

Initial research on activated carbon was directed towards increasing the pore volume by developing high SSA and refining the activation process. However, the capacitance increase was limited even for the most porous samples. From a series of activated carbons with different pore sizes in various electrolytes, it was shown that there was no linear relationship between the SSA and the capacitance^{19–21}. Some



Figure 3 Electrochemical capacitors. **a**, Schematic of a commercial spirally wound double layer capacitor. **b**, Assembled device weighing 500 g and rated for 2,600 F. (Photo courtesy of Batscap, Groupe Bolloré, France.) **c**, A small button cell, which is just 1.6 mm in height and stores 5 F. (Photo courtesy of Y-Carbon, US.) Both devices operate at 2.7 V.

studies suggested that pores smaller than 0.5 nm were not accessible to hydrated ions^{20,22} and that even pores under 1 nm might be too small, especially in the case of organic electrolytes, where the size of the solvated ions is larger than 1 nm (ref. 23). These results were consistent with previous work showing that ions carry a dynamic sheath of solvent molecules, the solvation shell²⁴, and that some hundreds of kilojoules per mole are required to remove it²⁵ in the case of water molecules. A pore size distribution in the range 2–5 nm, which is larger than the size of two solvated ions, was then identified as a way to improve the energy density and the power capability. Despite all efforts, only a moderate improvement has been made. Gravimetric capacitance in the range of 100–120 F g⁻¹ in organic and 150–200 F g⁻¹ in aqueous electrolytes has been achieved^{26,27} and ascribed to improved ionic mass transport inside mesopores. It was assumed that a well balanced micro- or mesoporosity (according to IUPAC classification, micropores are smaller than 2 nm, whereas mesopores are 2–50 nm in diameter) was needed to maximize capacitance²⁸.

Although fine-tuned mesoporous carbons failed to achieve high capacitance performance, several studies reported an important capacitive contribution from micropores. From experiments using activated carbon cloth, Salitra *et al.*²⁹ suggested that a partial desolvation of ions could occur, allowing access to small pores (<2 nm). High capacitance was observed for a mesoporous carbon containing large numbers of small micropores^{30–32}, suggesting that partial ion desolvation could lead to an improved capacitance. High capacitances (120 F g⁻¹ and 80 F cm⁻³) were found in organic electrolytes for microporous carbons (<1.5 nm)^{33,34}, contradicting the solvated ion adsorption theory. Using microporous activated coal-based carbon materials, Raymundo-Pinero *et al.*³⁵ observed the same effect and found a maximum capacitance for pore size at 0.7 and

0.8 nm for aqueous and organic electrolytes, respectively. However, the most convincing evidence of capacitance increase in pores smaller than the solvated ion size was provided by experiments using carbide-derived carbons (CDCs)^{36–38} as the active material. These are porous carbons obtained by extraction of metals from carbides (TiC, SiC and other) by etching in halogens at elevated temperatures³⁹:



In this reaction, Ti is leached out from TiC, and carbon atoms self-organize into an amorphous or disordered, mainly *sp*²-bonded⁴⁰, structure with a pore size that can be fine-tuned by controlling the chlorination temperature and other process parameters. Accordingly, a narrow uni-modal pore size distribution can be achieved in the range 0.6–1.1 nm, and the mean pore size can be controlled with sub-ångström accuracy⁴¹. These materials were used to understand the charge storage in micropores using 1 M solution of NEt₄BF₄ in acetonitrile-based electrolyte⁴². The normalized capacitance (μF cm⁻²) decreased with decreasing pore size until a critical value close to 1 nm was reached (Fig. 4), and then sharply increased when the pore size approached the ion size. As the CDC samples were exclusively microporous, the capacitance increase for subnanometre pores clearly shows the role of micropores. Moreover, the gravimetric and volumetric capacitances achieved by CDC were, respectively, 50% and 80% higher than for conventional activated carbon^{19–21}. The capacitance change with the current density was also found to be stable, demonstrating the high power capabilities these materials can achieve⁴². As the solvated ion sizes in this electrolyte were 1.3 and 1.16 nm for the cation and anion¹⁶, respectively, it was proposed that partial or complete removal of their solvation shell was allowing the ions to access the micropores. As a result, the change of capacitance was a linear function of 1/*b* (where *b* is the pore radius), confirming that the distance between the ion and the carbon surface, *d*, was shorter for the smaller pores. This dependence published by Chmiola *et al.*⁴² has since been confirmed by other studies, and analysis of literature data is provided in refs 43 and 44.

CHARGE-STORAGE MECHANISM IN SUBNANOMETRE PORES

From a fundamental point of view, there is a clear lack of understanding of the double layer charging in the confined space of micropores, where there is no room for the formation of the Helmholtz layer and diffuse layer expected at a solid–electrolyte interface. To address this issue, a three-electrode cell configuration, which discriminates between anion and cation adsorption, was used⁴⁵. The double layer capacitance in 1.5 M NEt₄BF₄-acetonitrile electrolyte caused by the anion and cation at the positive and negative electrodes, respectively, had maxima at different pore sizes⁴⁵. The peak in capacitance shifted to smaller pores for the smaller ion (anion). This behaviour cannot be explained by purely electrostatic reasons, because all pores in this study were the same size as or smaller than a single ion with a single associated solvent molecule. It thus confirmed that ions must be at least partially stripped of solvent molecules in order to occupy the carbon pores. These results point to a charge storage mechanism whereby partial or complete removal of the solvation shell and increased confinement of ions lead to increased capacitance.

A theoretical analysis published by Huang *et al.*⁴³ proposed splitting the capacitive behaviour in two different parts depending on the pore size. For mesoporous carbons (pores larger than 2 nm), the traditional model describing the charge of the double layer was used⁴³:

$$C/A = \frac{\epsilon_r \epsilon_0}{b \ln \left(\frac{b}{b-d} \right)} \quad (5)$$

where *b* is the pore radius and *d* is the distance of approach of the ion to the carbon surface. Data from Fig. 4 in the mesoporous range

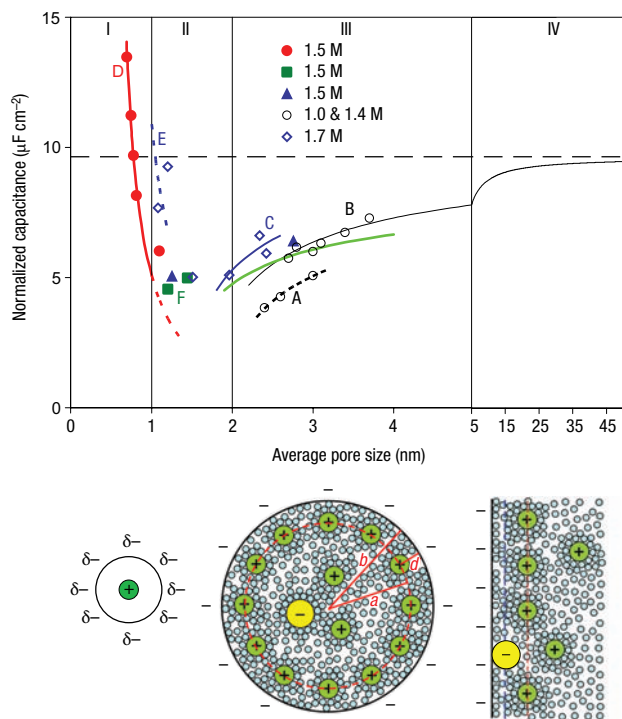


Figure 4 Specific capacitance normalized by SSA as a function of pore size for different carbon samples. All samples were tested in the same electrolyte ($\text{NEt}_4^+\text{BF}_4^-$ in acetonitrile; concentrations are shown in the key). Symbols show experimental data for CDCs, templated mesoporous carbons and activated carbons, and lines show model fits⁴³. A huge normalized capacitance increase is observed for microporous carbons with the smallest pore size in zone I, which would not be expected in the traditional view. The partial or complete loss of the solvation shell explains this anomalous behaviour⁴². As schematics show, zones I and II can be modelled as an electric wire-in-cylinder capacitor, an electric double-cylinder capacitor should be considered for zone III, and the commonly used planar electric double layer capacitor can be considered for larger pores, when the curvature/size effect becomes negligible (zone IV). A mathematical fit in the mesoporous range (zone III) is obtained using equation (5). Equation (6) was used to model the capacitive behaviour in zone I, where confined micropores force ions to desolvate partially or completely⁴⁴. A, B: templated mesoporous carbons; C: activated mesoporous carbon; D, F: microporous CDC; E: microporous activated carbon. Reproduced with permission from ref. 44. © 2008 Wiley.

(zone III) were fitted with equation (5). For micropores (<1 nm), it was assumed that ions enter a cylindrical pore and line up, thus forming the ‘electric wire in cylinder’ model of a capacitor. Capacitance was calculated from⁴³

$$C/A = \frac{\epsilon_r \epsilon_0}{b \ln\left(\frac{b}{a_0}\right)} \quad (6)$$

where a_0 is the effective size of the ion (desolvated). This model perfectly matches with the normalized capacitance change versus pore size (zone I in Fig. 4). Calculations using density functional theory gave consistent values for the size, a_0 , for unsolvated NEt_4^+ and BF_4^- ions⁴³.

This work suggests that removal of the solvation shell is required for ions to enter the micropores. Moreover, the ionic radius a_0 found by using equation (6) was close to the bare ion size, suggesting that ions could be fully desolvated. A study carried out with CDCs in a

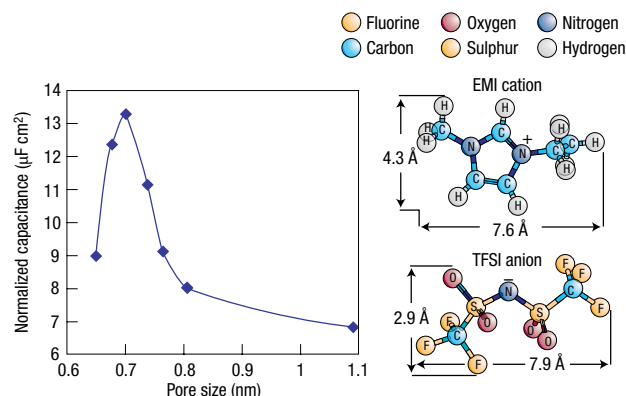


Figure 5 Normalized capacitance change as a function of the pore size of carbon-derived-carbide samples. Samples were prepared at different temperatures in ethyl-methylimidazolium/trifluoro-methane-sulphonylimide (EMI,TFSI) ionic liquid at 60 °C. Inset shows the structure and size of the EMI and TFSI ions. The maximum capacitance is obtained when the pore size is in the same range as the maximum ion dimension. Reproduced with permission from ref. 46. © 2008 ACS.

solvent-free electrolyte ($[\text{EMI}^+,\text{TFSI}^-]$ ionic liquid at 60 °C), in which both ions have a maximum size of about 0.7 nm, showed the maximum capacitance for samples with the 0.7-nm pore size⁴⁶, demonstrating that a single ion per pore produces the maximum capacitance (Fig. 5). This suggests that ions cannot be adsorbed on both pore surfaces, in contrast with traditional supercapacitor models.

MATERIALS BY DESIGN

The recent findings of the micropore contribution to the capacitive storage highlight the lack of fundamental understanding of the electrochemical interfaces at the nanoscale and the behaviour of ions confined in nanopores. In particular, the results presented above rule out the generally accepted description of the double layer with solvated ions adsorbed on both sides of the pore walls, consistent with the absence of a diffuse layer in subnanometre pores. Although recent studies^{45,46} provide some guidance for developing materials with improved capacitance, such as elimination of macro- and mesopores and matching the pore size with the ion size, further material optimization by Edisonian or combinatorial electrochemistry methods may take a very long time. The effects of many parameters, such as carbon bonding (sp versus sp^2 or sp^3), pore shape, defects or adatoms, are difficult to determine experimentally. Clearly, computational tools and atomistic simulation will be needed to help us to understand the charge storage mechanism in subnanometre pores and to propose strategies to design the next generation of high-capacitance materials and material–electrolyte systems⁴⁷. Recasting the theory of double layers in electrochemistry to take into account solvation and desolvation effects could lead to a better understanding of charge storage as well as ion transport in ECs and even open up new opportunities in areas such as biological ion channels and water desalination.

REDOX-BASED ELECTROCHEMICAL CAPACITORS

MECHANISM OF PSEUDO-CAPACITIVE CHARGE STORAGE

Some ECs use fast, reversible redox reactions at the surface of active materials, thus defining what is called the pseudo-capacitive behaviour. Metal oxides such as RuO_2 , Fe_3O_4 or MnO_2 (refs 48, 49), as well as electronically conducting polymers⁵⁰, have been extensively studied in the past decades. The specific pseudo-capacitance exceeds

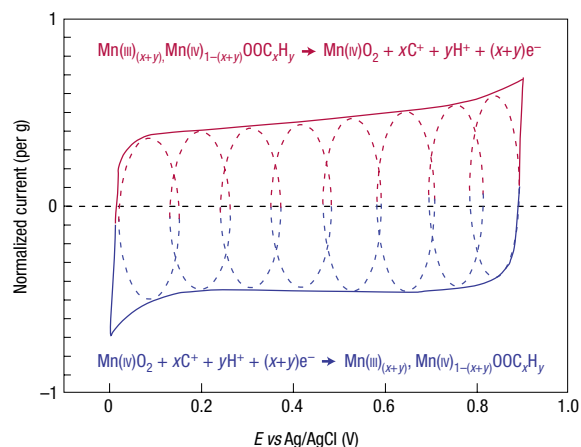


Figure 6 Cyclic voltammetry. This schematic of cyclic voltammetry for a MnO_2 -electrode cell in mild aqueous electrolyte (0.1 M K_2SO_4) shows the successive multiple surface redox reactions leading to the pseudo-capacitive charge storage mechanism. The red (upper) part is related to the oxidation from Mn(II) to Mn(IV) and the blue (lower) part refers to the reduction from Mn(IV) to Mn(II).

that of carbon materials using double layer charge storage, justifying interest in these systems. But because redox reactions are used, pseudo-capacitors, like batteries, often suffer from a lack of stability during cycling.

Ruthenium oxide, RuO_2 , is widely studied because it is conductive and has three distinct oxidation states accessible within 1.2 V. The pseudo-capacitive behaviour of RuO_2 in acidic solutions has been the focus of research in the past 30 years¹. It can be described as a fast, reversible electron transfer together with an electro-adsorption of protons on the surface of RuO_2 particles, according to equation (7), where Ru oxidation states can change from (II) up to (IV):



where $0 \leq x \leq 2$. The continuous change of x during proton insertion or de-insertion occurs over a window of about 1.2 V and leads to a capacitive behaviour with ion adsorption following a Frumkin-type isotherm¹. Specific capacitance of more than 600 F g^{-1} has been reported⁵¹, but Ru-based aqueous electrochemical capacitors are expensive, and the 1-V voltage window limits their applications to small electronic devices. Organic electrolytes with proton surrogates (for example Li^+) must be used to go past 1 V. Less expensive oxides of iron, vanadium, nickel and cobalt have been tested in aqueous electrolytes, but none has been investigated as much as manganese oxide⁵². The charge storage mechanism is based on surface adsorption of electrolyte cations C^+ (K^+ , Na^+ ...) as well as proton incorporation according to the reaction:

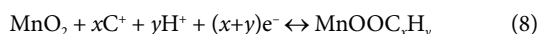


Figure 6 shows a cyclic voltammogram of a single MnO_2 electrode in mild aqueous electrolyte; the fast, reversible successive surface redox reactions define the behaviour of the voltammogram, whose shape is close to that of the EDLC. MnO_2 micro-powders or micrometre-thick films show a specific capacitance of about 150 F g^{-1} in neutral aqueous electrolytes within a voltage window of $<1 \text{ V}$. Accordingly, there is limited interest in MnO_2 electrodes for symmetric devices, because there are no oxidation states available at less than 0 V. However, it is suitable for a pseudo-capacitive positive electrode in hybrid systems,

which we will describe below. Other transition metal oxides with various oxidation degrees, such as molybdenum oxides, should also be explored as active materials for pseudo-capacitors.

Many kinds of conducting polymers (polyaniline, polypyrrole, polythiophene and their derivatives) have been tested in EC applications as pseudo-capacitive materials^{50,53,54} and have shown high gravimetric and volumetric pseudo-capacitance in various non-aqueous electrolytes at operating voltages of about 3 V. When used as bulk materials, conducting polymers suffer from a limited stability during cycling that reduces the initial performance⁹. Research efforts with conducting polymers for supercapacitor applications are nowadays directed towards hybrid systems.

NANOSTRUCTURING REDOX-ACTIVE MATERIALS TO INCREASE CAPACITANCE

Given that nanomaterials have helped to improve Li-ion batteries⁵⁵, it is not surprising that nanostructuring has also affected ECs. Because pseudo-capacitors store charge in the first few nanometres from the surface, decreasing the particle size increases active material usage. Thanks to a thin electrically conducting surface layer of oxide and oxynitride, the charging mechanism of nanocrystalline vanadium nitride (VN) includes a combination of an electric double layer and a faradic reaction (II/IV) at the surface of the nanoparticles, leading to specific capacitance up to $1,200 \text{ F g}^{-1}$ at a scan rate of 2 mV s^{-1} (ref. 56). A similar approach can be applied to other nano-sized transition metal nitrides or oxides. In another example, the cycling stability and the specific capacitance of RuO_2 nanoparticles were increased by depositing a thin conducting polymer coating that enhanced proton exchange at the surface⁵⁷. The design of specific surface functionalization to improve interfacial exchange could be suggested as a generic approach to other pseudo-redox materials.

MnO_2 and RuO_2 films have been synthesized at the nanometre scale. Thin MnO_2 deposits of tens to hundreds of nanometres have been produced on various substrates such as metal collectors, carbon nanotubes or activated carbons. Specific capacitances as high as $1,300 \text{ F g}^{-1}$ have been reported⁵⁸, as reaction kinetics were no longer limited by the electrical conductivity of MnO_2 . In the same way, Sugimoto's group have prepared hydrated RuO_2 nano-sheets with capacitance exceeding $1,300 \text{ F g}^{-1}$ (ref. 59). The RuO_2 specific capacitance also increased sharply when the film thickness was decreased. The deposition of RuO_2 thin film onto carbon supports^{60,61} both increased the capacitance and decreased the RuO_2 consumption. Thin film synthesis or high SSA capacitive material decoration with nano-sized pseudo-capacitive active material, like the examples presented in Fig. 7a and b, offers an opportunity to increase energy density and compete with carbon-based EDLCs. Particular attention must be paid to further processing of nano-sized powders into active films because they tend to re-agglomerate into large-size grains. An alternative way to produce porous films from powders is by growing nanotubes, as has been shown for V_2O_5 (ref. 62), or nanorods. These allow easy access to the active material, but can only be produced in thin films so far, and the manufacturing cost will probably limit the use of these sophisticated nanostructures to small electronic devices.

HYBRID SYSTEMS TO ACHIEVE HIGH ENERGY DENSITY

Hybrid systems offer an attractive alternative to conventional pseudo-capacitors or EDLCs by combining a battery-like electrode (energy source) with a capacitor-like electrode (power source) in the same cell. An appropriate electrode combination can even increase the cell voltage, further contributing to improvement in energy and power densities. Currently, two different approaches to hybrid systems have emerged: (i) pseudo-capacitive metal oxides with a capacitive carbon electrode, and (ii) lithium-insertion electrodes with a capacitive carbon electrode.

Numerous combinations of positive and negative electrodes have been tested in the past in aqueous or inorganic electrolytes. In most

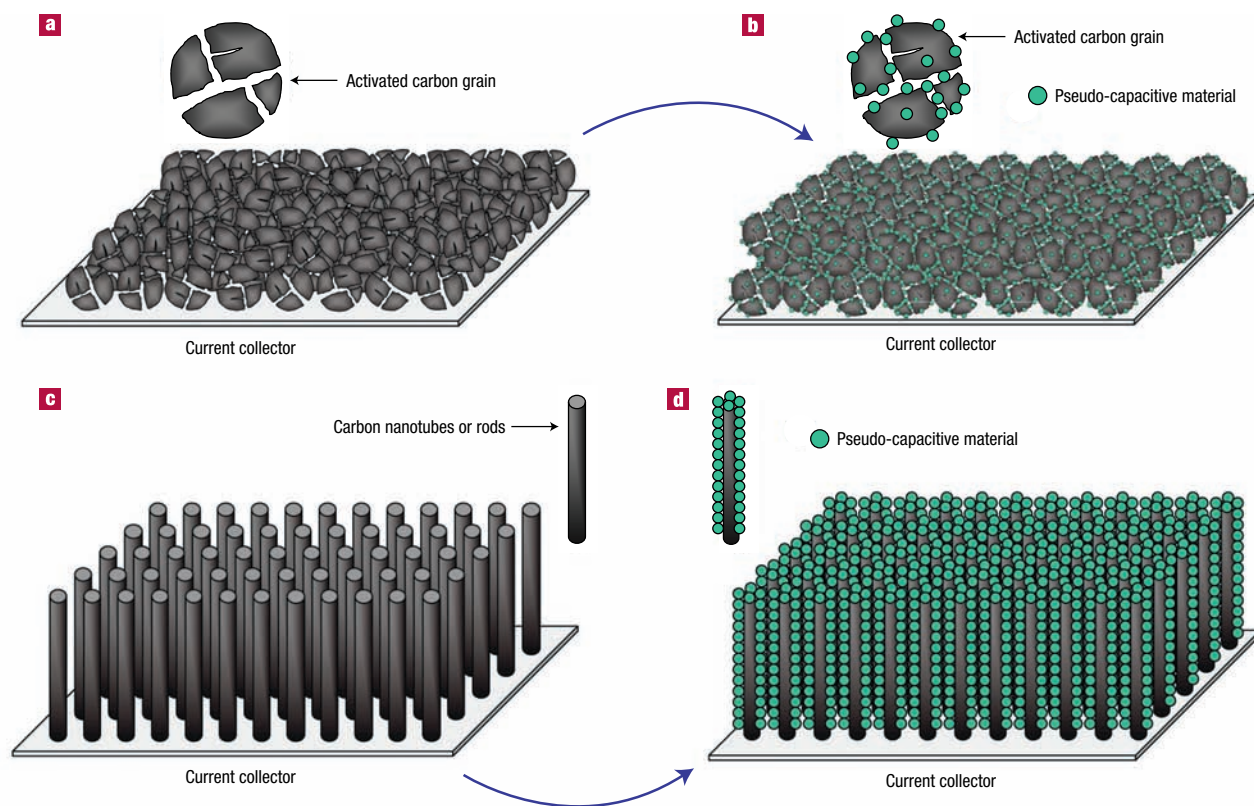


Figure 7 Possible strategies to improve both energy and power densities for electrochemical capacitors. **a, b**, Decorating activated carbon grains **(a)** with pseudo-capacitive materials **(b)**. **c, d**, Achieving conformal deposit of pseudo-capacitive materials **(d)** onto highly ordered high-surface-area carbon nanotubes **(c)**.

cases, the faradic electrode led to an increase in the energy density at the cost of cyclability (for balanced positive and negative electrode capacities). This is certainly the main drawback of hybrid devices, as compared with EDLCs, and it is important to avoid transforming a good supercapacitor into a mediocre battery⁶³.

MnO₂ is one of the most studied materials as a low-cost alternative to RuO₂. Its pseudo-capacitance arises from the III/IV oxidation state change at the surface of MnO₂ particles⁵⁸. The association of a negative EDLC-type electrode with a positive MnO₂ electrode leads to a 2-V cell in aqueous electrolytes thanks to the apparent water decomposition overvoltage on MnO₂ and high-surface-area carbon. The low-cost carbon–MnO₂ hybrid system combines high capacitance in neutral aqueous electrolytes with high cell voltages, making it a green alternative to EDLCs using acetonitrile-based solvents and fluorinated salts. Moreover, the use of MnO₂ nano-powders and nanostructures offers the potential for further improvement in capacitance⁶⁴. Another challenge for this system is to use organic electrolytes to reach higher cell voltage, thus improving the energy density.

A combination of a carbon electrode with a PbO₂ battery-like electrode using H₂SO₄ solution can work at 2.1 V (ref. 65), offering a low-cost EC device for cost-sensitive applications, in which weight of the device is of minor concern.

The hybrid concept originated from the Li-ion batteries field. In 1999, Amatucci's group combined a nanostructured lithium titanate anode Li₄Ti₅O₁₂ with an activated carbon positive electrode, designing a 2.8-V system that for the first time exceeded 10 Wh kg⁻¹ (ref. 66). The titanate electrode ensured high power capacity and no solid-electrolyte interphase formation, as well as long-life cyclability thanks to low volume change during cycling. Following this pioneering

work, many studies have been conducted on various combinations of a lithium-insertion electrode with a capacitive carbon electrode. The Li-ion capacitor developed by Fuji Heavy Industry is an example of this concept, using a pre-lithiated high SSA carbon anode together with an activated carbon cathode^{63,67}. It achieved an energy density of more than 15 Wh kg⁻¹ at 3.8 V. Capacity retention was increased by unbalancing the electrode capacities, allowing a low depth of charge/discharge at the anode. Systems with an activated carbon anode and anion intercalation cathode are also under development. The advent of nanomaterials⁵⁵ as well as fast advances in the area of Li-ion batteries should lead to the design of high-performance ECs. Combining newly developed high-rate conversion reaction anodes or Li-alloying anodes with a positive supercapacitor electrode could fill the gap between Li-ion batteries and EDLCs. These systems could be of particular interest in applications where high power and medium cycle life are needed.

CURRENT COLLECTORS

Because ECs are power devices, their internal resistance must be kept low. Particular attention must be paid to the contact impedance between the active film and the current collector. ECs designed for organic electrolytes use treated aluminium foil or grid current collectors. Surface treatments have already been shown to decrease ohmic drops at this interface⁶⁸, and coatings on aluminium that improve electrochemical stability at high potentials and interface conductivity are of great interest.

The design of nanostructured current collectors with an increased contact area is another way to control the interface between current

collector and active material. For example, carbon can be produced in a variety of morphologies¹², including porous films and nanotube brushes that can be grown on various current collectors⁶⁹ and that can serve as substrates for further conformal deposition (Fig. 7c and d) of active material. These nano-architected electrodes could outperform the existing systems by confining a highly pseudo-capacitive material to a thin film with a high SSA, as has been done for Li-ion batteries⁷⁰ where, by growing Cu nano-pillars on a planar Cu foil, a six-fold improvement in the energy density over planar electrodes has been achieved⁷⁰. Long's group⁶⁴ successfully applied a similar approach to supercapacitors by coating a porous carbon nano-foam with a 20-nm pseudo-capacitive layer of MnO₂. As a result, the area-normalized capacitance doubled to reach 1.5 F cm⁻², together with an outstanding volumetric capacitance of 90 F cm⁻³. Electrophoretic deposition from stable colloidal suspensions of RuO₂ (ref. 71) or other active material can be used for filling the inter-tube space to design high-energy-density devices which are just a few micrometres thick. The nano-architected electrodes also find applications in micro-systems where micro-ECs can complement micro-batteries for energy harvesting or energy generation. In this specific field, it is often advantageous to grow self-supported, binderless nano-electrodes directly on semiconductor wafers, such as Si or SiC (ref. 72; Fig. 2c).

An attractive material for current collectors is carbon in the form of a highly conductive nanotube or graphene paper. It does not corrode in aqueous electrolytes and is very flexible. The use of nanotube paper for manufacturing flexible supercapacitors is expected to grow as the cost of small-diameter nanotubes required for making paper decreases. The same thin sheet of nanotubes¹⁴ could potentially act as an active material and current collector at the same time. Thin-film, printable and wearable ECs could find numerous applications.

FROM ORGANIC TO IONIC LIQUID ELECTROLYTES

EC cell voltage is limited by the electrolyte decomposition at high potentials. Accordingly, the larger the electrolyte stability voltage window, the higher the supercapacitor cell voltage. Moving from aqueous to organic electrolytes increased the cell voltage from 0.9 V to 2.5–2.7 V for EDLCs. Because the energy density is proportional to the voltage squared (equation (2)), numerous research efforts have been directed at the design of highly conducting, stable electrolytes with a wider voltage window. Today, the state of the art is the use of organic electrolyte solutions in acetonitrile or propylene carbonate, the latter becoming more popular because of the low flash point and lower toxicity compared with acetonitrile.

Ionic liquids are room-temperature liquid solvent-free electrolytes; their voltage window stability is thus only driven by the electrochemical stability of the ions. A careful choice of both the anion and the cation allows the design of high-voltage supercapacitors, and 3-V, 1,000-F commercial devices are already available⁷³. However, the ionic conductivity of these liquids at room temperature is just a few milliSiemens per centimetre, so they are mainly used at higher temperatures. For example, CDC with an EMI/TFSI ionic liquid electrolyte has been shown⁴⁶ to have capacitance of 160 F g⁻¹ and ~90 F cm⁻³ at 60 °C. In this area, hybrid activated carbon/conducting polymer devices also show an improved performance with cell voltages higher than 3 V (refs 74–76).

For applications in the temperature range –30 °C to +60 °C, where batteries and supercapacitors are mainly used, ionic liquids still fail to satisfy the requirements because of their low ionic conductivity. However, the choice of a huge variety of combinations of anions and cations offers the potential for designing an ionic liquid electrolyte with an ionic conductivity of 40 mS cm⁻¹ and a voltage window of >4 V at room temperature⁷⁷. A challenge is, for instance, to find an alternative to the imidazolium cation that, despite high conductivity,

undergoes a reduction reaction at potential <1.5 V versus Li⁺/Li. Replacing the heavy bis(trifluoromethanesulphonyl)imide (TFSI) anion by a lighter (fluoromethanesulphonyl)imide (FSI) and preparing ionic liquid eutectic mixtures would improve both the cell voltage (because a protecting layer of AlF₃ can be formed on the Al surface, shifting the de-passivation potential of Al above 4 V) and the ionic conductivity⁷⁷. However, FSI shows poor cyclability at elevated temperatures. Supported by the efforts of the Li-ion community to design safer systems using ionic liquids, the research on ionic liquids for ECs is expected to have an important role in the improvement of capacitor performance in the coming years.

APPLICATIONS OF ELECTROCHEMICAL CAPACITORS

ECs are electrochemical energy sources with high power delivery and uptake, with an exceptional cycle life. They are used when high power demands are needed, such as for power buffer and power saving units, but are also of great interest for energy recovery. Recent articles from Miller *et al.*^{7,10} present an overview of the opportunities for ECs in a variety of applications, complementing an earlier review by Kötz *et al.*⁹. Small devices (a few farads) are widely used for power buffer applications or for memory back-up in toys, cameras, video recorders, mobile phones and so forth. Cordless tools such as screwdrivers and electric cutters using EDLCs are already available on the market. Such systems, using devices of a few tens of farads, can be fully charged or discharged in less than 2 minutes, which is particularly suited to these applications, with the cycle life of EDLC exceeding that of the tool. As mentioned before, the Airbus A380 jumbo jets use banks of EDLCs for emergency door opening. The modules consist of an in series/parallel assembly of 100-F, 2.7-V cells that are directly integrated into the doors to limit the use of heavy copper cables. This application is obviously a niche market, but it is a demonstration that the EDLC technology is mature in terms of performance, reliability and safety.

The main market targeted by EDLC manufacturers for the next years is the transportation market, including hybrid electric vehicles, as well as metro trains and tramways. There continues to be debate about the advantage of using high power Li-ion batteries instead of ECs (or vice versa) for these applications. Most of these discussions have been initiated by Li-ion battery manufacturers who would like their products to cover the whole range of applications. However, ECs and Li-ion batteries should not necessarily be seen as competitors, because their charge storage mechanisms and thus their characteristics are different. The availability of the stored charge will always be faster for a supercapacitor (surface storage) than for a Li-ion battery (bulk storage), with a larger stored energy for the latter. Both devices must be used in their respective time-constant domains (see Fig. 1). Using a Li-ion battery for repeated high power delivery/uptake applications for a short duration (10 s or less) will quickly degrade the cycle life of the system¹⁰. The only way to avoid this is to oversize the battery, increasing the cost and volume. In the same way, using ECs for power delivery longer than 10 s requires oversizing. However, some applications use ECs as the main power and energy source, benefiting from the fast charge/discharge capability of these systems as well as their outstanding cycle life. Several train manufacturers have clearly identified the tramway/metro market segment as extremely relevant for EC use, to power trains over short distances in big cities, where electric cables are clearly undesirable for aesthetic and other reasons, but also to recover the braking energy of another train on the same line, thanks to the ECs' symmetric high power delivery/uptake characteristics.

For automotive applications, manufacturers are already proposing solutions for electrical power steering, where ECs are used for load-leveling in stop-and-go traffic⁷⁸. The general trend is to increase the hybridization degree of the engines in hybrid electric vehicles, to allow fast acceleration (boost) and braking energy recovery. The

on-board energy storage systems will be in higher demand, and a combination of batteries and EDLCs will increase the battery cycle life, explaining why EDLCs are viewed as a partner to Li-ion batteries for this market⁷⁸. Currently, high price limits the use of both Li-ion batteries and EDLC in large-scale applications (for example for load levelling). But the surprisingly high cost of materials used for EDLC is due to a limited number of suppliers rather than intrinsically high cost of porous carbon. Decreasing the price of carbon materials for ECs, including CDC and AC, would remove the main obstacle to their wider use⁷⁹.

SUMMARY AND OUTLOOK

The most recent advances in supercapacitor materials include nanoporous carbons with the pore size tuned to fit the size of ions of the electrolyte with ångström accuracy, carbon nanotubes for flexible and printable devices with a short response time, and transition metal oxide and nitride nanoparticles for pseudo-capacitors with a high energy density. An improved understanding of charge storage and ion desolvation in subnanometre pores has helped to overcome a barrier that has been hampering progress in the field for decades. It has also shown how important it is to match the active materials with specific electrolytes and to use a cathode and anode with different pore sizes that match the anion or cation size. Nano-architecture of electrodes has led to further improvements in power delivery. The very large number of possible active materials and electrolytes means that better theoretical guidance is needed for the design of future ECs.

Future generations of ECs are expected to come close to current Li-ion batteries in energy density, maintaining their high power density. This may be achieved by using ionic liquids with a voltage window of more than 4 V, by discovering new materials that combine double-layer capacitance and pseudo-capacitance, and by developing hybrid devices. ECs will have a key role in energy storage and harvesting, decreasing the total energy consumption and minimizing the use of hydrocarbon fuels. Capacitive energy storage leads to a lower energy loss (higher cycle efficiency), than for batteries, compressed air, flywheel or other devices, helping to improve storage economy further. Flexible, printable and wearable ECs are likely to be integrated into smart clothing, sensors, wearable electronics and drug delivery systems. In some instances they will replace batteries, but in many cases they will either complement batteries, increasing their efficiency and lifetime, or serve as energy solutions where an extremely large number of cycles, long lifetime and fast power delivery are required.

doi:10.1038/nmat2297

References

- Conway, B. E. *Electrochemical Supercapacitors: Scientific Fundamentals and Technological Applications* (Kluwer, 1999).
- Service, R. F. New 'supercapacitor' promises to pack more electrical punch. *Science* **313**, 902–905 (2007).
- Tarascon, J.-M. & Armand, M. Issues and challenges facing rechargeable lithium batteries. *Nature* **414**, 359–367 (2001).
- Brodd, R. J. *et al.* Batteries, 1977 to 2002. *J. Electrochem. Soc.* **151**, K1–K11 (2004).
- Armand, M. & Tarascon, J.-M. Building better batteries. *Nature* **451**, 652–657 (2008).
- Armand, M. & Johansson, P. Novel weakly coordinating heterocyclic anions for use in lithium batteries. *J. Power Sources* **178**, 821–825 (2008).
- Miller, J. R. & Simon, P. Electrochemical capacitors for energy management. *Science* **321**, 651–652 (2008).
- US Department of Energy. *Basic Research Needs for Electrical Energy Storage* <www.sc.doe.gov/bes/reports/abstracts.html#EES2007> (2007).
- Kötz, R. & Carlen, M. Principles and applications of electrochemical capacitors. *Electrochim. Acta* **45**, 2483–2498 (2000).
- Miller, J. R. & Burke, A. F. Electrochemical capacitors: Challenges and opportunities for real-world applications. *Electrochem. Soc. Interf.* **17**, 53–57 (2008).
- Pandolfo, A. G. & Hollenkamp, A. F. Carbon properties and their role in supercapacitors. *J. Power Sources* **157**, 11–27 (2006).
- Gogotsi, Y. (ed.) *Carbon Nanomaterials* (CRC, 2006).
- Kyotani, T., Chmiola, J. & Gogotsi, Y. in *Carbon Materials for Electrochemical Energy Storage Systems* (eds Beguin, F. & Frackowiak, E.) Ch. 13 (CRC/Taylor and Francis, in the press).
- Futaba, D. N. *et al.* Shape-engineerable and highly densely packed single-walled carbon nanotubes and their application as super-capacitor electrodes. *Nature Mater.* **5**, 987–994 (2006).
- Portet, C., Chmiola, J., Gogotsi, Y., Park, S. & Lian, K. Electrochemical characterizations of carbon nanomaterials by the cavity microelectrode technique. *Electrochim. Acta* **53**, 7675–7680 (2008).
- Yang, C.-M. *et al.* Nanowindow-regulated specific capacitance of supercapacitor electrodes of single-wall carbon nanohorns. *J. Am. Chem. Soc.* **129**, 20–21 (2007).
- Niu, C., Sichel, E. K., Hoch, R., Moy, D. & Tennent, H. High power electrochemical capacitors based on carbon nanotube electrodes. *Appl. Phys. Lett.* **70**, 1480 (1997).
- Azaïs, P. *et al.* Causes of supercapacitors ageing in organic electrolyte. *J. Power Sources* **171**, 1046–1053 (2007).
- Gamby, J., Taberna, P. L., Simon, P., Fauvarque, J. F. & Chesneau, M. Studies and characterization of various activated carbons used for carbon/carbon supercapacitors. *J. Power Sources* **101**, 109–116 (2001).
- Shi, H. Activated carbons and double layer capacitance. *Electrochim. Acta* **41**, 1633–1639 (1995).
- Qu, D. & Shi, H. Studies of activated carbons used in double-layer capacitors. *J. Power Sources* **74**, 99–107 (1998).
- Qu, D. Studies of the activated carbons used in double-layer supercapacitors. *J. Power Sources* **109**, 403–411 (2002).
- Kim, Y. J. *et al.* Correlation between the pore and solvated ion size on capacitance uptake of PVDC-based carbons. *Carbon* **42**, 1491 (2004).
- Izutsu, K. *Electrochemistry in Nonaqueous Solution* (Wiley, 2002).
- Marcus, Y. *Ion Solvation* (Wiley, 1985).
- Jurewicz, K. *et al.* Capacitance properties of ordered porous carbon materials prepared by a templating procedure. *J. Phys. Chem. Solids* **65**, 287 (2004).
- Fernández, J. A. *et al.* Performance of mesoporous carbons derived from poly(vinyl alcohol) in electrochemical capacitors. *J. Power Sources* **175**, 675 (2008).
- Fuertes, A. B., Lota, G., Centeno, T. A. & Frackowiak, E. Templated mesoporous carbons for supercapacitor application. *Electrochim. Acta* **50**, 2799 (2005).
- Salitra, G., Soffer, A., Eliad, L., Cohen, Y. & Aurbach, D. Carbon electrodes for double-layer capacitors. I. Relations between ion and pore dimensions. *J. Electrochem. Soc.* **147**, 2486–2493 (2000).
- Vix-Guterl, C. *et al.* Electrochemical energy storage in ordered porous carbon materials. *Carbon* **43**, 1293–1302 (2005).
- Eliad, L., Salitra, G., Soffer, A. & Aurbach, D. On the mechanism of selective electroadsorption of protons in the pores of carbon molecular sieves. *Langmuir* **21**, 3198–3202 (2005).
- Eliad, L. *et al.* Assessing optimal pore-to-ion size relations in the design of porous poly(vinylidene chloride) carbons for EDL capacitors. *Appl. Phys. A* **82**, 607–613 (2006).
- Arulepp, M. *et al.* The advanced carbide-derived carbon based supercapacitor. *J. Power Sources* **162**, 1460–1466 (2006).
- Arulepp, M. *et al.* Influence of the solvent properties on the characteristics of a double layer capacitor. *J. Power Sources* **133**, 320–328 (2004).
- Raymundo-Pinero, E., Kierzek, K., Machnikowski, J. & Beguin, F. Relationship between the nanoporous texture of activated carbons and their capacitance properties in different electrolytes. *Carbon* **44**, 2498–2507 (2006).
- Janes, A. & Lust, E. Electrochemical characteristics of nanoporous carbide-derived carbon materials in various nonaqueous electrolyte solutions. *J. Electrochem. Soc.* **153**, A113–A116 (2006).
- Shanina, B. D. *et al.* A study of nanoporous carbon obtained from ZC powders (Z = Si, Ti, and B). *Carbon* **41**, 3027–3036 (2003).
- Chmiola, J., Dash, R., Yushin, G. & Gogotsi, Y. Effect of pore size and surface area of carbide derived carbon on specific capacitance. *J. Power Sources* **158**, 765–772 (2006).
- Dash, R. *et al.* Titanium carbide derived nanoporous carbon for energy-related applications. *Carbon* **44**, 2489–2497 (2006).
- Urbanaitis, S. *et al.* EELS studies of carbide derived carbons. *Carbon* **45**, 2047–2053 (2007).
- Gogotsi, Y. *et al.* Nanoporous carbide-derived carbon with tunable pore size. *Nature Mater.* **2**, 591–594 (2003).
- Chmiola, J. *et al.* Anomalous increase in carbon capacitance at pore size below 1 nm. *Science* **313**, 1760–1763 (2006).
- Huang, J. S., Sumpter, B. G. & Meunier, V. Theoretical model for nanoporous carbon supercapacitors. *Angew. Chem. Int. Ed.* **47**, 520–524 (2008).
- Huang, J., Sumpter, B. G. & Meunier, V. A universal model for nanoporous carbon supercapacitors applicable to diverse pore regimes, carbons, and electrolytes. *Chem. Eur. J.* **14**, 6614–6626 (2008).
- Chmiola, J., Largeot, C., Taberna, P.-L., Simon, P. & Gogotsi, Y. Desolvation of ions in subnanometer pores, its effect on capacitance and double-layer theory. *Angew. Chem. Int. Ed.* **47**, 3392–3395 (2008).
- Largeot, C. *et al.* Relation between the ion size and pore size for an electric double-layer capacitor. *J. Am. Chem. Soc.* **130**, 2730–2731 (2008).
- Weigand, G., Davenport, J. W., Gogotsi, Y. & Roberto, J. in *Scientific Impacts and Opportunities for Computing Ch.* 5, 29–35 (DOE Office of Science, 2008).
- Wu, N.-L. Nanocrystalline oxide supercapacitors. *Mater. Chem. Phys.* **75**, 6–11 (2002).
- Brousse, T. *et al.* Crystalline MnO₂ as possible alternatives to amorphous compounds in electrochemical supercapacitors. *J. Electrochem. Soc.* **153**, A2171–A2180 (2006).
- Rudge, A., Raistrick, I., Gottesfeld, S. & Ferraris, J. P. Conducting polymers as active materials in electrochemical capacitors. *J. Power Sources* **47**, 89–107 (1994).
- Zheng, J. P. & Jow, T. R. High energy and high power density electrochemical capacitors. *J. Power Sources* **62**, 155–159 (1996).
- Lee, H. Y. & Goodenough, J. B. Supercapacitor behavior with KCl electrolyte. *J. Solid State Chem.* **144**, 220–223 (1999).
- Laforge, A., Simon, P. & Fauvarque, J.-F. Chemical synthesis and characterization of fluorinated polyphenylthiophenes: application to energy storage. *Synth. Met.* **123**, 311–319 (2001).
- Naoi, K., Suematsu, S. & Manago, A. Electrochemistry of poly(1,5-diaminoanthraquinone) and its application to electrochemical capacitor materials. *J. Electrochem. Soc.* **147**, 420–426 (2000).
- Arico, A. S., Bruce, P., Scrosati, B., Tarascon, J.-M. & Schalkwijk, W. V. Nanostructured materials for advanced energy conversion and storage devices. *Nature Mater.* **4**, 366–377 (2005).
- Choi, D., Blomgren, G. E. & Kumta, P. N. Fast and reversible surface redox reaction in nanocrystalline vanadium nitride supercapacitors. *Adv. Mater.* **18**, 1178–1182 (2006).

57. Machida, K., Furuuchi, K., Min, M. & Naoi, K. Mixed proton–electron conducting nanocomposite based on hydrous RuO₂ and polyaniline derivatives for supercapacitors. *Electrochemistry* **72**, 402–404 (2004).
58. Toupin, M., Brousse, T. & Belanger, D. Charge storage mechanism of MnO₂ electrode used in aqueous electrochemical capacitor. *Chem. Mater.* **16**, 3184–3190 (2004).
59. Sugimoto, W., Iwata, H., Yasunaga, Y., Murakami, Y. & Takasu, Y. Preparation of ruthenic acid nanosheets and utilization of its interlayer surface for electrochemical energy storage. *Angew. Chem. Int. Ed.* **42**, 4092–4096 (2003).
60. Miller, J. M., Dunn, B., Tran, T. D. & Pekala, R. W. Deposition of ruthenium nanoparticles on carbon aerogels for high energy density supercapacitor electrodes. *J. Electrochem. Soc.* **144**, L309–L311 (1997).
61. Min, M., Machida, K., Jang, J. H. & Naoi, K. Hydrous RuO₂/carbon black nanocomposites with 3D porous structure by novel incipient wetness method for supercapacitors. *J. Electrochem. Soc.* **153**, A334–A338 (2006).
62. Wang, Y., Takahashi, K., Lee, K. H. & Cao, G. Z. Nanostructured vanadium oxide electrodes for enhanced lithium-ion intercalation. *Adv. Funct. Mater.* **16**, 1133–1144 (2006).
63. Naoi, K. & Simon, P. New materials and new configurations for advanced electrochemical capacitors. *Electrochem. Soc. Interf.* **17**, 34–37 (2008).
64. Fischer, A. E., Pettigrew, K. A., Rolison, D. R., Stroud, R. M. & Long, J. W. Incorporation of homogeneous, nanoscale MnO₂ within ultraporos carbon structures via self-limiting electroless deposition: Implications for electrochemical capacitors. *Nano Lett.* **7**, 281–286 (2007).
65. Kazaryan, S. A., Razumov, S. N., Litvinenko, S. V., Kharisov, G. G. & Kogan, V. I. Mathematical model of heterogeneous electrochemical capacitors and calculation of their parameters. *J. Electrochem. Soc.* **153**, A1655–A1671 (2006).
66. Amatucci, G. G., Badway, F. & DuPasquier, A. in *Intercalation Compounds for Battery Materials* (ECS Proc. Vol. 99) 344–359 (Electrochemical Society, 2000).
67. Burke, A. R&D considerations for the performance and application of electrochemical capacitors. *Electrochim. Acta* **53**, 1083–1091 (2007).
68. Portet, C., Taberna, P. L., Simon, P. & Laberty-Robert, C. Modification of Al current collector surface by sol-gel deposit for carbon-carbon supercapacitor applications. *Electrochim. Acta* **49**, 905–912 (2004).
69. Talapatra, S. *et al.* Direct growth of aligned carbon nanotubes on bulk metals. *Nature Nanotech.* **1**, 112–116 (2006).
70. Taberna, L., Mitra, S., Poizat, P., Simon, P. & Tarascon, J. M. High rate capabilities Fe₃O₄-based Cu nano-architected electrodes for lithium-ion battery applications. *Nature Mater.* **5**, 567–573 (2006).
71. Jang, J. H., Machida, K., Kim, Y. & Naoi, K. Electrophoretic deposition (EPD) of hydrous ruthenium oxides with PTFE and their supercapacitor performances. *Electrochim. Acta.* **52**, 1733 (2006).
72. Cambaz, Z. G., Yushin, G., Osswald, S., Mochalin, V. & Gogotsi, Y. Noncatalytic synthesis of carbon nanotubes, graphene and graphite on SiC. *Carbon* **46**, 841–849 (2008).
73. Tsuda, T. & Hussey, C. L. Electrochemical applications of room-temperature ionic liquids. *Electrochem. Soc. Interf.* **16**, 42–49 (2007).
74. Balducci, A. *et al.* High temperature carbon–carbon supercapacitor using ionic liquid as electrolyte. *J. Power Sources* **165**, 922–927 (2007).
75. Balducci, A. *et al.* Cycling stability of a hybrid activated carbon//poly(3-methylthiophene) supercapacitor with *N*-butyl-*N*-methylpyrrolidinium bis(trifluoromethanesulfonyl)imide ionic liquid as electrolyte. *Electrochim. Acta* **50**, 2233–2237 (2005).
76. Balducci, A., Soavi, F. & Mastragostino, M. The use of ionic liquids as solvent-free green electrolytes for hybrid supercapacitors. *Appl. Phys. A* **82**, 627–632 (2006).
77. Endres, F., MacFarlane, D. & Abbott, A. (eds) *Electrodeposition from Ionic Liquids* (Wiley-VCH, 2008).
78. Faggioli, E. *et al.* Supercapacitors for the energy management of electric vehicles. *J. Power Sources* **84**, 261–269 (1999).
79. Chmiola, J. & Gogotsi, Y. Supercapacitors as advanced energy storage devices. *Nanotechnol. Law Bus.* **4**, 577–584 (2007).
80. Portet, C., Yushin, G. & Gogotsi, Y. Electrochemical performance of carbon onions, nanodiamonds, carbon black and multiwalled nanotubes in electrical double layer capacitors. *Carbon* **45**, 2511–2518 (2007).

Acknowledgements

We thank our students and collaborators, including J. Chmiola, C. Portet, R. Dash and G. Yushin (Drexel University), P. L. Taberna and C. Largeot (Université Paul Sabatier), and J. E. Fischer (University of Pennsylvania) for experimental help and discussions, H. Burnside (Drexel University) for editing the manuscript and S. Cassou (Toulouse) for help with illustrations. This work was partially funded through the Department of Energy, Office of Basic Energy Science, grant DE-FG01-05ER05-01, and through the Délégation Générale pour l'Armement.

Nanostructured materials for advanced energy conversion and storage devices

New materials hold the key to fundamental advances in energy conversion and storage, both of which are vital in order to meet the challenge of global warming and the finite nature of fossil fuels. Nanomaterials in particular offer unique properties or combinations of properties as electrodes and electrolytes in a range of energy devices. This review describes some recent developments in the discovery of nanoelectrolytes and nanoelectrodes for lithium batteries, fuel cells and supercapacitors. The advantages and disadvantages of the nanoscale in materials design for such devices are highlighted.

**ANTONINO SALVATORE ARICÒ¹,
PETER BRUCE², BRUNO SCROSATI^{3*},
JEAN-MARIE TARASCON⁴ AND
WALTER VAN SCHALKWIJK⁵**

¹Istituto CNR-ITAE, 98126 S. Lucia, Messina, Italy

²School of Chemistry, University of St Andrews, KY16 9ST, Scotland

³Dipartimento di Chimica, Università 'La Sapienza', 00186 Rome, Italy

⁴Université de Picardie Jules Verne, LRCs; CNRS UMR-6047, 80039 Amiens, France

⁵EnergyPlex Corporation, 1400 SE 112th Avenue, Suite 210, Bellevue, Washington 98004, USA

*e-mail: scrosati@uniroma1.it

One of the great challenges in the twenty-first century is unquestionably energy storage. In response to the needs of modern society and emerging ecological concerns, it is now essential that new, low-cost and environmentally friendly energy conversion and storage systems are found; hence the rapid development of research in this field. The performance of these devices depends intimately on the properties of their materials. Innovative materials chemistry lies at the heart of the advances that have already been made in energy conversion and storage, for example the introduction of the rechargeable lithium battery. Further breakthroughs in materials, not incremental changes, hold the key to new generations of energy storage and conversion devices.

Nanostructured materials have attracted great interest in recent years because of the unusual mechanical, electrical and optical properties endowed by confining the dimensions of such materials and because of the combination of bulk and surface properties to the overall behaviour. One

need only consider the staggering developments in microelectronics to appreciate the potential of materials with reduced dimensions. Nanostructured materials are becoming increasingly important for electrochemical energy storage^{1,2}. Here we address this topic. It is important to appreciate the advantages and disadvantages of nanomaterials for energy conversion and storage, as well as how to control their synthesis and properties. This is a sizeable challenge facing those involved in materials research into energy conversion and storage. It is beyond the scope of this review to give an exhaustive summary of the energy storage and conversion devices that may now or in the future benefit from the use of nanoparticles; rather, we shall limit ourselves to the fields of lithium-based batteries, supercapacitors and fuel cells. Furthermore, from now on we shall refer to nanomaterials composed of particles that are of nanometre dimensions as primary nanomaterials, and those for which the particles are typically of micrometre dimensions but internally consist of nanometre-sized regions or domains as secondary nanomaterials.

LITHIUM BATTERIES

Lithium-ion batteries are one of the great successes of modern materials electrochemistry³. Their science and technology have been extensively reported in previous reviews⁴ and dedicated books^{5,6}, to which the reader is referred for more details. A lithium-ion battery consists of a lithium-ion intercalation negative electrode (generally graphite), and a lithium-ion intercalation positive electrode (generally the lithium metal oxide, LiCoO₂), these being separated by a lithium-ion conducting electrolyte, for example a solution of LiPF₆ in ethylene carbonate-diethylcarbonate. Although such batteries are commercially successful, we are reaching the limits in performance using the

current electrode and electrolyte materials. For new generations of rechargeable lithium batteries, not only for applications in consumer electronics but especially for clean energy storage and use in hybrid electric vehicles, further breakthroughs in materials are essential. We must advance the science to advance the technology. When such a situation arises, it is important to open up new avenues. One avenue that is already opening up is that of nanomaterials for lithium-ion batteries

ELECTRODES

There are several potential advantages and disadvantages associated with the development of nanoelectrodes for lithium batteries. Advantages include (i) better accommodation of the strain of lithium insertion/removal, improving cycle life; (ii) new reactions not possible with bulk materials; (iii) higher electrode/electrolyte contact area leading to higher charge/discharge rates; (iv) short path lengths for electronic transport (permitting operation with low electronic conductivity or at higher power); and (v) short path lengths for Li^+ transport (permitting operation with low Li^+ conductivity or higher power). Disadvantages include (i) an increase in undesirable electrode/electrolyte reactions due to high surface area, leading to self-discharge, poor cycling and calendar life; (ii) inferior packing of particles leading to lower volumetric energy densities unless special compaction methods are developed; and (iii) potentially more complex synthesis.

With these advantages and disadvantages in mind, efforts have been devoted to exploring negative and, more recently, positive nanoelectrode materials.

ANODES

Metals that store lithium are among the most appealing and competitive candidates for new types of anodes (negative electrodes) in lithium-ion batteries. Indeed, a number of metals and semiconductors, for example aluminium, tin and silicon, react with lithium to form alloys by electrochemical processes that are partially reversible and of low voltage (relative to lithium), involve a large number of atoms per formula unit, and in particular provide a specific capacity much larger than that offered by conventional graphite^{7,8}. For example, the lithium-silicon alloy has, in its fully lithiated composition, $\text{Li}_{4.4}\text{Si}$, a theoretical specific capacity of $4,200 \text{ mA h g}^{-1}$ compared with $3,600 \text{ mA h g}^{-1}$ for metallic lithium and 372 mA h g^{-1} for graphite. Unfortunately, the accommodation of so much lithium is accompanied by enormous volume changes in the host metal plus phase transitions. The mechanical strain generated during the alloying/de-alloying processes leads to cracking and crumbling of the metal electrode and a marked loss of capacity to store charge, in the course of a few cycles^{8,9}.

Although these structural changes are common to alloying reactions, there have been attempts to limit their side effects on the electrode integrity. Among them, the active/inactive nanocomposite concept

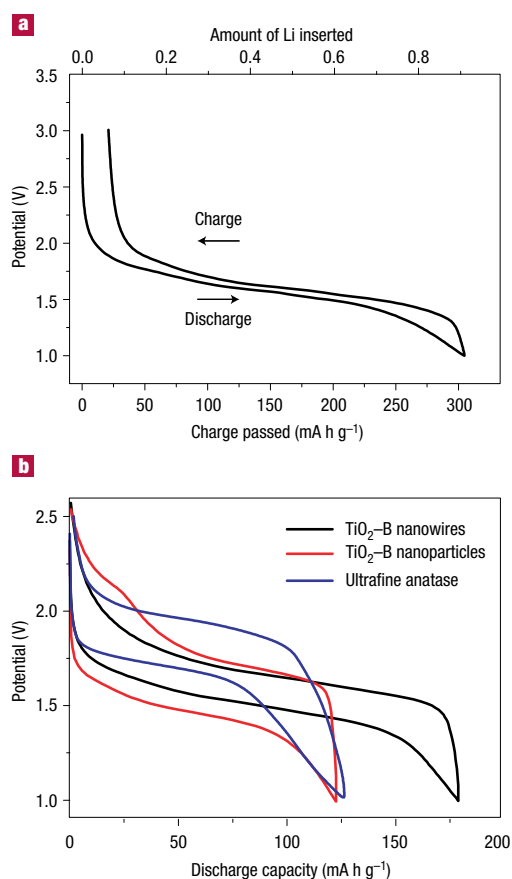


Figure 1 Charge–discharge curves for nanostructured anode materials.

a, Charge–discharge curves for $\text{Li}_x\text{TiO}_2\text{-B}$ nanowires (rate of 10 mA g^{-1}). **b**, Comparison of cycling behaviour for $\text{TiO}_2\text{-B}$ nanowires, $\text{TiO}_2\text{-B}$ nanoparticles and nanoparticulate anatase, all at 200 mA g^{-1} .

represents one attractive route. Several authors^{7–9} have discussed this approach, which involves intimately mixing two materials, one reacting with lithium whereas the other acts as an inactive confining buffer. Within this composite, the use of nano-size metallic clusters as lithium hosts considerably suppresses the associated strains, and therefore improves the reversibility of the alloying reaction. By applying this concept through different systems such as SnO-based glasses¹⁰, or composites such as Sn–Fe–C (ref. 11), Sn–Mn–C (ref. 12) or Si–C (refs 13–15), several authors have demonstrated that these electrodes show a considerable improvement in their cycling response in lithium cells. The Si–C nanocomposites have attracted considerable interest because they show capacity as high as $1,000 \text{ mA h g}^{-1}$ for more than 100 cycles¹⁵. Some of these improvements may arise because the materials avoid cracking, thus maintaining better conduction pathways, or because they incorporate conductive additives such as carbon. Undoubtedly alloy performance can also benefit from nanostructuring. For instance, thin amorphous silicon films deposited on a specially roughened copper foil surface by a sputtering process were shown¹⁶ to have close to 100% reversibility at capacities larger than $3,000 \text{ mA h g}^{-1}$. An excellent capacity retention was also noted for silicon electrodes prepared with a nanopillar surface morphology¹⁷ because size confinement alters particle deformation and reduces fracturing.

Table 1 The Gibbs free energy change ΔG of conversion reactions. Values are obtained using thermodynamic data given in the literature²² for various compounds together with the corresponding electromotive force (e.m.f.) values E , as deduced from the well-known $\Delta G = -nEF$ where F is Faraday's constant.

Compound		ΔG (kg mol ⁻¹)	E (V) = E_{eq} (volts vs Li ⁺ /Li ⁰)
CoS _{0.89}	(+2)	-265.5	1.73
CoO	(+2)	-347.0	1.79
CoCl ₂	(+2)	-499.0	2.59
CoF ₂	(+2)	-528.2	2.74
CoF ₃	(+3)	-1,023.4	3.54

Perhaps the greatest disadvantage of primary nanoparticles is the possibility of significant side-reactions with the electrolyte, leading to safety concerns (one of the most critical issues for lithium batteries) and poor calendar life. But if the materials fall within the stability window of the electrolyte or at least limit the formation of the solid–electrolyte interface (SEI) layer, then the many advantages of nanoparticles may more easily be exploited. Such an example is Li_{4+x}Ti₅O₁₂ ($0 < x < 3$, 160 mA h g⁻¹, 1.6 V versus Li⁺(1M)/Li). No evidence has been reported for a significant surface layer formation (presumably because the potential is sufficiently high compared with lithium), and this material can be used as a nanoparticulate anode with high rate capability and good capacity retention. Controlling the nanoparticle shape as well as size can offer advantages. This is illustrated by recent results on TiO₂-B nanotubes or wires (B designates the form of TiO₂ and not boron). Such materials may be synthesized by a simple aqueous route and in high yield, with diameters in the range of 40–60 nm and lengths up to several micrometres. The TiO₂-B polymorph is an excellent intercalation host for Li, accommodating up to Li_{0.91}TiO₂-B (305 mA h g⁻¹) at 1.5–1.6 V vs Li⁺(1M)/Li and with excellent capacity retention on cycling (Fig. 1). Interestingly, the rate capability is better than the same phase prepared as nanoparticles of dimension similar to the diameter of the nanowires¹⁸ (Fig. 1). These TiO₂-B electrodes are not the only nanotube/wire electrodes. Unsurprisingly, carbon nanotubes have been explored as anodes. Whether the cost of their synthesis is viable remains an open question.

Nanomaterials consisting of nanoparticles or nanoarchitected materials, as described so far in this review, are not always easy to make because of difficulties in controlling the size and size distribution of the particles or clusters. The potential disadvantage of a high external surface area, leading to excessive side reactions with the electrolyte and hence capacity losses or poor calendar life, has already been mentioned. Such problems may be addressed with internally nanostructured materials (secondary nanomaterials as defined), where the particles are significantly larger than the nanodomains. As well as

reducing side reactions with the electrolyte, this can have the advantage of ensuring higher volumetric energy densities. Of course, as described below, they are not a panacea.

A group of internally nanostructured anodes based on transition metal oxides has recently been described. The full electrochemical reduction of oxides such as CoO, CuO, NiO, Co₃O₄ and MnO versus lithium, involving two or more electrons per 3d-metal, was shown to lead to composite materials consisting of nanometre-scale metallic clusters dispersed in an amorphous Li₂O matrix¹⁹. Owing to the nanocomposite nature of these electrodes, the reactions, termed 'conversion reactions', are highly reversible, providing large capacities that can be maintained for hundreds of cycles. The prevailing view had been that reversible lithium reaction could occur only in the presence of crystal structures with channels able to transport Li⁺. The new results, in stark contrast, turn out not to be specific to oxides but can be extended to sulphides, nitrides or fluorides²⁰. These findings help to explain the previously reported unusual reactivity of complex oxides including RVO₄ (R = In, Fe) or A_xMoO₃ towards lithium^{21,22}.

Such conversion reactions offer numerous opportunities to 'tune' the voltage and capacity of the cell¹⁹ owing to the fact that the cell potential is directly linked to the strength of the M–X bonding. Weaker M–X bonding gives larger potentials. The capacity is directly linked to the metal oxidation state, with the highest capacity associated with the highest oxidation states. Thus, by selecting the nature of M and its oxidation state, as well as the nature of the anion, one can obtain reactions with a specific potential within the range 0 to 3.5 V (Table 1), and based on low-cost elements such as Mn or Fe. Fluorides generally yield higher potentials than oxides, sulphides and nitrides.

However, such excitement needs to be tempered because ensuring rapid and reversible nanocomposite reactions is not an easy task. The future of such conversion reactions in real-life applications lies in mastering their kinetics (for example, the chemical diffusion of lithium into the matrix). Great progress has already been achieved with oxides, especially metallic RuO₂, which was shown²³ to display a 100% reversible conversion process involving 4e⁻, and some early but encouraging results have been reported with

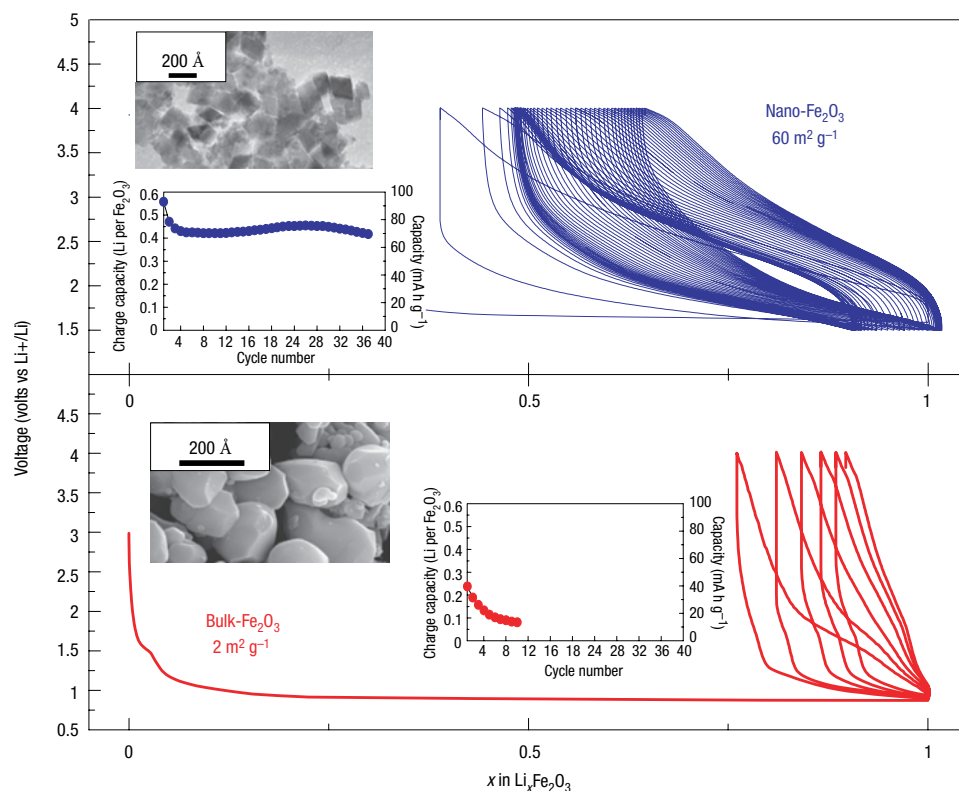


Figure 2 Electrochemical behaviour of bulk and nanostructured $\alpha\text{-Fe}_2\text{O}_3$ with voltage–composition curves. The capacity retention and scanning electron micrographs of both samples are shown in the insets.

fluorides^{24–26}; but a great deal remains to be done in this area. A further hint that working at the nanoscale may radically change chemical/electrochemical reaction paths of inorganic materials comes from recent studies carried out on the reactivity of macroscopic versus nanoscale haematite ($\alpha\text{-Fe}_2\text{O}_3$) particles with Li. With nanometre-scale haematite particles (20 nm), reversible insertion of 0.6 Li per Fe_2O_3 is possible through a single-phase process, whereas large haematite particles (1 to 2 μm) undergo an irreversible phase transformation as soon as ~ 0.05 Li per Fe_2O_3 are reacted (see Fig. 2)²⁷. In this respect, many materials, previously rejected because they did not fulfil the criteria as classical intercalation hosts for lithium, are now worth reconsideration.

CATHODES

This area is much less developed than the nanoanodes. The use of nanoparticulate forms (primary nanomaterials) of the classical cathode materials such as LiCoO_2 , LiNiO_2 or their solid solutions can lead to greater reaction with the electrolyte, and ultimately more safety problems, especially at high temperatures, than the use of such materials in the micrometre range. In the case of Li–Mn–O cathodes such as LiMn_2O_4 , the use of small particles increases undesirable dissolution of Mn. Coating the particles with a stabilizing surface layer may help to alleviate such problems but can reduce the rate of intercalation, reducing the advantage of the small particles.

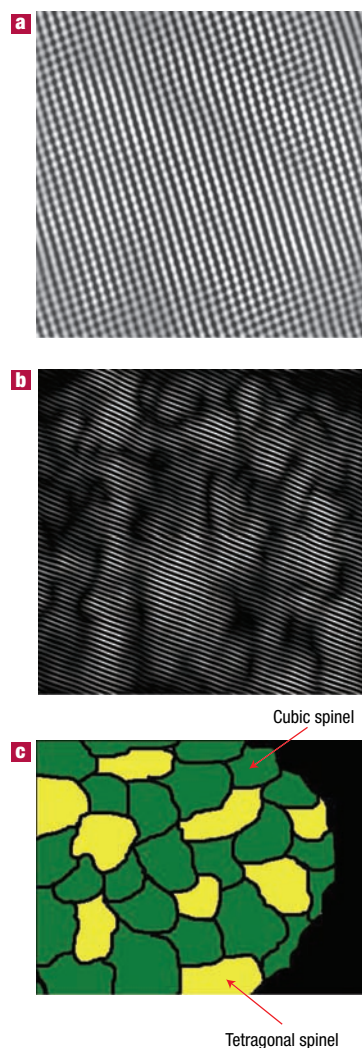
A related approach to the formation of silicon

nanopillars has been taken for cathode materials. By using a template, for example, porous alumina or a porous polymer, nanopillars of V_2O_5 or LiMn_2O_4 have been grown on a metal substrate²⁸. These microfabricated electrode structures have the advantages of the Si example, accommodating volume changes and supporting high rates, although in the case of the manganese oxide, accelerated dissolution is expected. Nanotubes of VO_x have also been prepared and investigated as cathodes²⁹.

Tuning the electrode material morphology or texture to obtain porous and high-surface-area electrodes constitutes another route to enhance electrode capacities³⁰. For V_2O_5 , aerogels (disordered mesoporous materials with a high pore volume) were recently reported to have electroactive capacities greater than polycrystalline non-porous V_2O_5 powders³¹. Such aerogels present a large surface area to the electrolyte, and can support high rates, although cyclability can be a problem because of structural changes or very reactive surface groups.

Interesting developments in secondary particle cathodes for lithium batteries have taken place in parallel with the work on secondary particle anodes. By retaining large particles, there is less dissolution than with primary nanoparticulate materials, and high volumetric densities are retained. Conventional wisdom stated that to sustain rapid and reversible electrode reactions in rechargeable lithium batteries, intercalation compounds must be used as the electrodes, and that the intercalation process had to be single-phase, that is, a continuous solid solution on

Figure 3 Transmission electron micrographs of regular and nanostructured spinel. **a**, Regular $\text{Li}_x\text{Mn}_{2-y}\text{O}_4$ spinel. **b**, $\text{Li}_x\text{Mn}_{2-y}\text{O}_4$ spinel obtained on cycling layered (O3) $\text{Li}_x\text{Mn}_{1-y}\text{O}_2$. The Fourier-filtered image (**b**) highlights the nanodomain structure of average dimensions 50–70 Å. **c**, A schematic representation of the nanodomain structure of $\text{Li}_x\text{Mn}_{2-y}\text{O}_4$ spinel derived from layered $\text{Li}_x\text{Mn}_{1-y}\text{O}_2$, showing cubic and tetragonal nanodomains.



intercalation. However, there are now many examples where lithium intercalation is facile despite undergoing phase transitions, including LiCoO_2 and $\text{Li}_4\text{Ti}_5\text{O}_{12}$, especially if there is a strong structural similarity between the end phases (for example, only differences in Li ordering). Such two-phase intercalation reactions are far from being universally reversible. A classic example³² is the intercalation cathode $\text{Li}_x\text{Mn}_2\text{O}_4$, $0 < x < 2$. Cycling is usually confined to the range $0 < x < 1$ to avoid the transformation of cubic LiMn_2O_4 to tetragonal $\text{Li}_2\text{Mn}_2\text{O}_4$, which leads to a marked loss of capacity (ability to cycle lithium) because of the 13% anisotropy in the lattice parameters on formation of the tetragonal phase. Layered LiMnO_2 with the $\alpha\text{-NaFeO}_2$ structure transforms into spinel on cycling but may be cycled with >99.9% capacity retention, despite undergoing the same cubic–tetragonal transformation³³. The reason is clearly not suppression of the Jahn–Teller driven cubic–tetragonal distortion (something that has been attempted many times with limited success). Instead, the system accommodates the strain associated with the

transformation by developing a nanostructure within the micrometre-sized particles (Fig. 3). The nanodomains of spinel switch between cubic and tetragonal structures, with the strain being accommodated by slippage at the domain wall boundaries^{34,35}. The nanodomains form during the layered-to-spinel transformation. Subsequently it has been shown that such a nanostructure can be induced in normal spinel by grinding, with a similar enhancement in cyclability³⁶. Interestingly, the layered-to-spinel transformation is very easy, helping to mitigate any ill effects the transformation itself may have on cyclability³⁷.

A further, somewhat different, example of the benefits of nanoelectrodes within the field of batteries is the optimization of the environmentally benign and low-cost phospho-olivine LiFePO_4 phase³⁸ that displays a theoretical capacity of 170 mA h g^{-1} , as compared with 140 mA h g^{-1} for the LiCoO_2 electrode used at present (LiFePO_4 operates at a lower voltage). But the insulating character of the olivine means that in practice one could not obtain the full capacity of the material because, as the electrochemical reaction proceeds, ‘electronically’ isolated areas remain inactive in the bulk electrode. As a result, this material was largely ignored until it was prepared in the form of carbon-coated nanoparticles (Fig. 4) through various chemical and physical means^{39–41}. This simultaneously reduces the distance for Li^+ transport, and increases the electronic contact between the particles. Procedures of this kind have led to a greatly improved electrochemical response, and the full capacity of the material is now accessible even under prolonged cycling³⁹ (see also Fig. 4). This example serves to illustrate some of the advantages of nanoelectrode materials listed at the beginning of this section, and to demonstrate that the search for new electroactive materials is now wider than ever because such materials do not require a particularly high electronic conductivity, nor a high diffusion coefficient for lithium, as had been believed for the past 20 years.

ELECTROLYTES

Progress in lithium batteries relies as much on improvements in the electrolyte as it does on the electrodes. Solid polymer electrolytes represent the ultimate in terms of desirable properties for batteries because they can offer an all-solid-state construction, simplicity of manufacture, a wide variety of shapes and sizes, and a higher energy density (because the constituents of the cell may be more tightly wound). No corrosive or explosive liquids can leak out, and internal short-circuits are less likely, hence greater safety. The most desirable polymer electrolytes are those formed by solvent-free membranes, for example poly(ethylene oxide), PEO, and a lithium salt, LiX , for example LiPF_6 or LiCF_3SO_3 (ref. 42). The poor ionic conductivity of these materials at room temperature has prevented them from realizing their otherwise high promise. Dispersing nanoscale inorganic fillers in solvent-free, polyether-based electrolytes increases the

conductivity several-fold^{43–45}. The improvement of the electrolyte transport properties may be explained on the basis of the heterogeneous doping model developed by Maier⁴⁶. Accordingly, nanocomposites can be defined as the distribution of a second (or even third) phase, with particles of nanometric dimension in a matrix that can be amorphous or crystalline. Thus the increase in conductivity may be associated with Lewis acid–base interactions between the surface states of the ceramic nanoparticle with both the polymer chains and the anion of the lithium salt⁴⁷. As in the electrode case, there are of course pros and cons in this particular approach. Indeed, other avenues are being explored to achieve high-conductivity polymer electrolytes. Relevant in this respect are the polymer-in-salt nanostructures⁴⁸ and the role of ionic liquids⁴⁹.

For 30 years it has been accepted that ionic conductivity in polymer electrolytes occurred exclusively in the amorphous phase, above the glass transition temperature T_g . Crystalline polymer electrolytes were considered to be insulators. But recent studies have shown that this is not the case: the 6:1 crystalline complexes PEO₆:LiXF₆; X = P, As, Sb demonstrate ionic conductivity^{50,51}. The Li⁺ ions reside in tunnels formed by the polymer chains (Fig. 5). Significant increases in ionic conductivity in the crystalline 6:1 complexes are observed on reducing the chain length from 3,000 to 1,000: that is, in the nanometre range⁵². It is evident that in electrolytes, just as in the electrodes described above, control of dimensions on the nanoscale has a profound influence on performance⁵². Crystalline polymer electrolytes represent a radically different type of ionic conductivity in polymers, and illustrate the importance of seeking new scientific directions. The present materials do not support ionic conductivities that are sufficient for applications, but they do offer a fresh approach with much scope for further advances. Recently it has been shown that the conductivity of the crystalline polymer electrolytes may be raised by two orders of magnitude by partial replacement of the XF₆ ions with other mono or divalent anions (ref. 53, and P. G. Bruce, personal communication). Chemical compatibility with selected electrode materials has yet to be evaluated.

SUPERCAPACITORS

Supercapacitors are of key importance in supporting the voltage of a system during increased loads in everything from portable equipment to electric vehicles^{54–56}. These devices occupy the area in the Ragone plot (that is, the plot of volumetric against gravimetric energy density) between batteries and dielectric capacitors. Supercapacitors are similar to batteries in design and manufacture (two electrodes, separator and electrolyte), but are designed for high power and long cycle life (>100 times battery life), but at the expense of energy density.

There are two general categories of electrochemical supercapacitors: electric double-layer capacitors (EDLC) and redox supercapacitors. In contrast to batteries, where the cycle life is limited

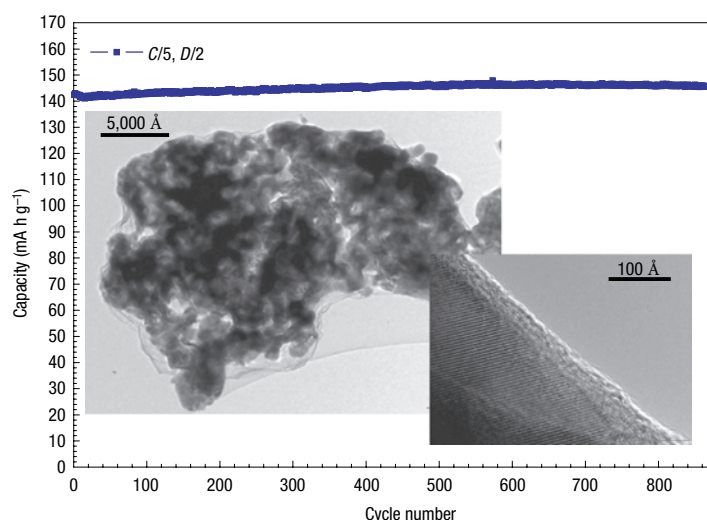


Figure 4 Capacity against cycling number for a lithium coin cell. The experiments used a 1-cm² disc of Bellcore-type plastic laminate made out 4.480 mg of pure LiFePO₄ coated with 5% C *in situ*. The overall plastic composition was 69% LiFePO₄, 11% C total and 20% Kynar. The cell was cycled at C/5 (0.160 mA cm⁻²), D/2 (–0.400 mA cm⁻²) between 2 and 4.5 V at room temperature. Here, D is discharge rate, C is charge rate. Left inset: enlarged transmission electron micrograph of the LiFePO₄ particles used, coated with carbon. The coating used a homemade recipe¹⁰³. This image was recorded with a TECNAI F20 scanning TEM. The quality of the coating — that is, the interface between crystallized LiFePO₄ and amorphous carbon — is nicely observed in the high-resolution electron micrograph in the right inset (taken with the same microscope). Courtesy of C. Wurm and C. Masquelier, LRCS Amiens.

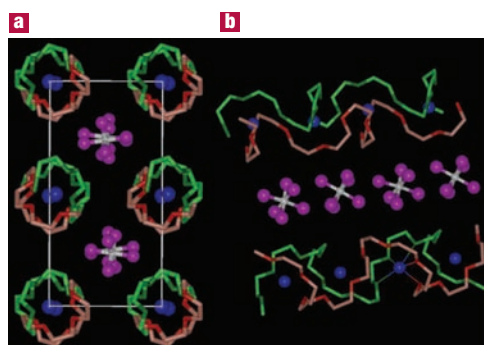
because of the repeated contraction and expansion of the electrode on cycling, EDLC lifetime is in principle infinite, as it operates solely on electrostatic surface-charge accumulation. For redox supercapacitors, some fast faradic charge transfer takes place as in a battery. This gives rise to a large pseudo-capacitance.

Progress in supercapacitor technology can benefit by moving from conventional to nanostructured electrodes. In the case of supercapacitors, the electrode requirements are less demanding than in batteries, at least in terms of electrode compaction, because power prevails over energy density. Thus, the benefits of nanopowders with their high surface area (primary nanoparticles) are potentially more important, hence the staggering interest in nanopowders and their rapid uptake for supercapacitor-based storage sources.

Recent trends in supercapacitors involve the development of high-surface-area activated carbon electrodes to optimize the performance in terms of capacitance and overall conductivity. Attention has been focused on nanostructured carbons, such as aerogels⁵⁷, nanotubes⁵⁸ and nanotemplates⁵⁹. The advantages of carbon aerogels lie mainly in their low ionic and electronic charging resistance and in their potential use as binderless electrodes. Replacing the standard carbon fibre with carbon aerogel electrodes improves capacitance and cyclability. Because of their unique architecture, carbon nanotubes are now intensively studied as new electrode materials for supercapacitor structures although, as for batteries, cost may be an issue. A critical aspect in nanotechnology for supercapacitors is to reach a compromise between specific surface area (to ensure high capacitance) and pore-size distribution (to permit easy access for the electrolyte).

Nanostructured materials have led to the development of new supercapacitor technologies. Capitalizing on the benefits of nanomaterial electrodes, Telcordia's researchers have, by means of the so-called hybrid supercapacitors (HSCs), proposed a new approach to energy storage⁶⁰. HSCs use one capacitive carbon electrode similar to that of a carbon EDLC; however, the complementary negative electrode consists of a nanostructured lithium

Figure 5 The structures of $\text{PEO}_6 \cdot \text{LiAsF}_6$. **a**, View of the structure along a showing rows of Li^+ ions perpendicular to the page. **b**, View of the structure showing the relative position of the chains and its conformation (hydrogens not shown). Thin lines indicate coordination around the Li^+ cation. Blue spheres, lithium; white spheres, arsenic; magenta, fluorine; green, carbon; red, oxygen.



titanate compound that undergoes a reversible faradic intercalation reaction⁶¹. The key innovation lies in the use of a nanostructured $\text{Li}_4\text{Ti}_5\text{O}_{12}$ as the negative electrode, resulting in no degradation in performance from charge/discharge-induced strain. Here is a nanomaterial that is being explored for capacitor and battery use because of its excellent cyclability, rate capability and safety. Its use in the hybrid supercapacitor results in a device with cycle life comparable to that of supercapacitors, freeing designers from the lifespan limitations generally associated with batteries. Figure 6 shows some features of these new types of capacitors. Besides $\text{Li}_4\text{Ti}_5\text{O}_{12}$, other nanostructured oxide materials can be engineered so as to obtain hybrid devices operating over a wide range of voltages. Inorganic nanotubes or nanowires may offer an alternative to nanoparticulate $\text{Li}_4\text{Ti}_5\text{O}_{12}$, for example the Li_xTiO_2 -B nanowires described in the section on lithium batteries. One can therefore envisage a supercapacitor composed of a carbon nanotube as the positive electrode and an inorganic nanotube capable of lithium intercalation (for example Li_xTiO_2 -B) as the negative electrode.

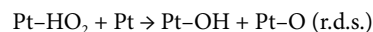
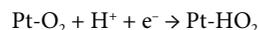
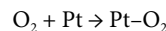
Fabricating nanopillared electrodes by growing the materials on a substrate was described in the context of lithium batteries. However, a related approach where materials are electro-synthesized in the presence of an electrolyte, which is also a liquid-crystal template, has been used to form nanoarchitected electrodes, for example Ni or NiOOH, for possible use in supercapacitors⁶¹.

FUEL CELLS

Fuel cell technologies are now approaching commercialization, especially in the fields of portable power sources — distributed and remote generation of electrical energy⁶². Already, nanostructured materials are having an impact on processing methods in the development of low-temperature fuel cells ($T < 200^\circ\text{C}$), the dispersion of precious metal catalysts, the development and dispersion of non-precious catalysts, fuel reformation and hydrogen storage, as well as the fabrication of membrane-electrode assemblies (MEA). Polymer electrolyte membrane fuel cells (PEMFCs) have recently gained momentum for application in transportation and as small portable power sources; whereas phosphoric acid fuel cells (PAFCs), solid oxide fuel cells (SOFCs) and molten carbonates fuel

cells (MCFCs) still offer advantages for stationary applications, and especially for co-generation⁶². Platinum-based catalysts are the most active materials for low-temperature fuel cells fed with hydrogen, reformat or methanol⁶². To reduce the costs, the platinum loading must be decreased (while maintaining or improving MEA performance), and continuous processes for fabricating MEAs in high volume must be developed. A few routes are being actively investigated to improve the electrocatalytic activity of Pt-based catalysts. They consist mainly of alloying Pt with transition metals or tailoring the Pt particle size.

The oxygen reduction reaction (ORR) limits the performance of low-temperature fuel cells. One of the present approaches in order to increase the catalyst dispersion involves the deposition of Pt nanoparticles on a carbon black support. Kinoshita *et al.* observed that the mass activity and specific activity for oxygen electro-reduction in acid electrolytes varies with the Pt particle size according to the relative fraction of Pt surface atoms on the (111) and (100) faces⁶³ (Fig. 7). The mass-averaged distribution of the surface atoms on the (111) and (100) planes passes through a maximum ($\sim 3\text{ nm}$) whereas the total fraction of surface atoms at the edge and corner sites decreases rapidly with an increase of the particle size. On the other hand, the surface-averaged distribution for the (111) and (100) planes shows a rapid increase with the particle size, which accounts for the increase of the experimentally determined specific activity with the particle size (Fig. 7). A dual-site reaction is assumed as the rate-determining step:

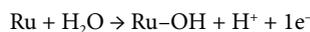


This mechanism accounts for the role of dual sites of proper orientation⁶³.

Alloying Pt with transition metals also enhances the electrocatalysis of O_2 reduction. In low-temperature fuel cells, Pt-Fe, Pt-Cr and Pt-Cr-Co alloy electrocatalysts were observed^{62,64,65} to have high specific activities for oxygen reduction as compared with that on platinum. This enhancement in electrocatalytic activity has been ascribed to several factors such as interatomic spacing, preferred orientation or electronic interactions. The state of the art Pt-Co-Cr electrocatalysts have a particle size of 6 nm (ref. 65).

Both CO_2 and CO are present in hydrogen streams obtained from reforming. These molecules are known to adsorb on the Pt surface under reducing potentials. Adsorbed CO-like species are also formed on Pt-based anode catalysts in direct methanol fuel cells (DMFCs). Such a poisoning of the Pt surface reduces the electrical efficiency and the power density of the fuel cell⁶⁶. The electrocatalytic activity of Pt against, for example, CO_2/CO poisoning is known to be promoted by the presence of a second metal^{64,65,67}, such as Ru, Sn or Mo. The mechanism by which such synergistic promotion of the H_2/CO and methanol

oxidation reactions is brought about has been much studied and is still debated. Nevertheless, it turns out that the best performance is obtained from Pt–Ru electrocatalysts with mean particle size 2–3 nm. As in the case of oxygen reduction, the particle size is important for structure-sensitive reactions such as CH₃OH and CO electro-oxidation. The catalytic activity of Pt–Ru surfaces is maximized for the (111) crystallographic plane⁶⁸. According to the bifunctional theory, the role of Ru in these processes is to promote water discharge and removal of strongly adsorbed CO species at low potentials through the following reaction mechanism^{66–68}:



A change in the CO binding strength to the surface induced by Ru through a ligand effect on Pt has been reported^{66,67}.

The synthesis of Pt-based electro-catalysts, either unsupported or supported on high-surface-area carbon, is generally carried out by various colloidal preparation routes. A method recently developed by Bönemann and co-workers⁶⁷ allows fine-tuning of the particle size for the bimetallic Pt–Ru system.

Recent developments in the field of CO-tolerant catalysts include the synthesis of new nanostructures by spontaneous deposition of Pt sub-monolayers on carbon-supported Ru nanoparticles^{68,69}. This also seems to be an efficient approach to reduce the Pt loading. Further advances concern a better understanding of the surface chemistry in electrocatalyst nanoparticles and the effects of strong metal–support interactions that influence both the dispersion and electronic nature of platinum sites.

An alternative approach, avoiding the use of carbon blacks, is the fabrication of porous silicon catalyst support structures with a 5- μm pore diameter and a thickness of about 500 μm . These structures have high surface areas, and they are of interest for miniature PEM fuel cells⁷⁰. A finely dispersed, uniform distribution of nanometre-scale catalyst particles deposited on the walls of the silicon pores creates, in contact with the ionomer, an efficient three-phase reaction zone capable of high power generation in DMFCs⁷⁰.

As an alternative to platinum, organic transition metal complexes — for example, iron or cobalt organic macrocycles from the families of phenylporphyrins⁷¹ and nanocrystalline transition metal chalcogenides⁷² — are being investigated for oxygen reduction, especially in relation to their high selectivity towards the ORR and tolerance to methanol cross-over in DMFCs. The metal–organic macrocycle is supported on high-surface-area carbon, and treated at high temperatures (from 500 to 800 °C) to form a nanostructured compound that possesses a specific geometrical arrangement of atoms. These materials show suitable electrocatalytic activity, even if smaller than that of Pt, without any degradation in performance⁷¹.

As for batteries, the electrolyte is a key component of the fuel cell assembly. Perfluorosulphonic polymer

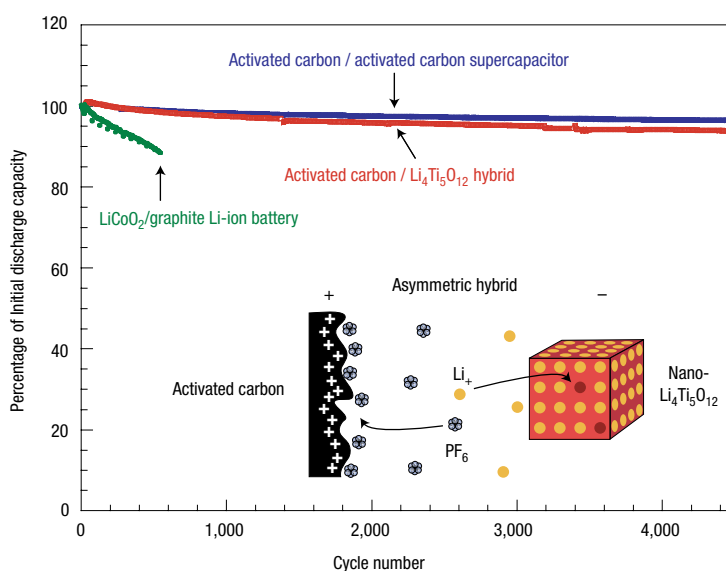


Figure 6 Cycling performance of the new asymmetric hybrid C/nano-Li₄Ti₅O₁₂ supercapacitor. Shown for comparison are results for a classical C/C supercapacitor and a commercial lithium-ion battery. The basic concept of this new type of supercapacitor is shown as an inset.

electrolyte membranes (for example Nafion™) are currently used in H₂/air or methanol/air fuel cells because of their excellent conductivity and electrochemical stability⁶². Unfortunately, they suffer from several drawbacks such as methanol cross-over and membrane dehydration. The latter severely hinders the fuel cell operation above 100 °C, which is a prerequisite for the suitable oxidation of small organic molecules involving formation of strongly adsorbed reaction intermediates such as CO-like species^{63,66,67}. Alternative membranes based on poly(arylene ether sulphone)⁷³, sulphonated poly(ether ketone)⁷⁴ or block co-polymer ion-channel-forming materials as well as acid-doped polyacrylamid and polybenzimidazole have been suggested^{75–77}. Various relationships between membrane nanostructure and transport characteristics, including conductivity, diffusion, permeation and electro-osmotic drag, have been observed⁷⁸. Interestingly, the presence of less-connected hydrophilic channels and larger separation of sulphonic groups in sulphonated poly(ether ketone) than in Nafion reduces water permeation and electro-osmotic drag whilst maintaining high protonic conductivity⁷⁸. Furthermore, an improvement in thermal and mechanical stability has been shown in nano-separated acid–base polymer blends obtained by combining polymeric N-bases and polymeric sulphonic acids⁷⁴. Considerable efforts have been addressed in the last decade to the development of composite membranes. These include ionomeric membranes modified by dispersing inside their polymeric matrix insoluble acids, oxides, zirconium phosphate and so on; other examples are ionomers or inorganic solid acids with high proton conductivity, embedded in porous non-proton-conducting polymers⁷⁵. Recently, Alberti and Casciola⁷⁵ prepared nanocomposite electrolytes by *in situ* formation of insoluble layered Zr phosphonates in ionomeric membranes. Such compounds, for example Zr(O₃P–OH)(O₃P–C₆H₄–SO₃H), show conductivities much higher than the Zr phosphates and comparable to Nafion. In an attempt to reduce

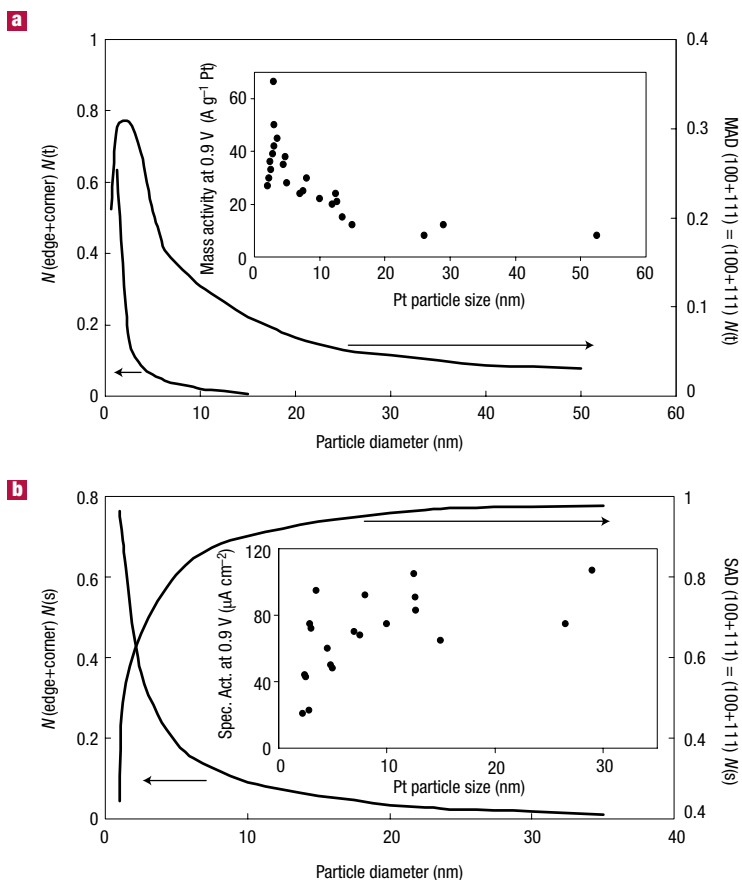


Figure 7 Calculated mass-averaged (a) and surface-averaged distributions (b) as a function of particle size in Pt particles with cubo-octahedral geometry. The values of $M(t)$ and $M(s)$ indicate the total number of atoms and the number of atoms on the surface respectively. The variation with particle size of mass activity (a) and specific activity (b) for oxygen reduction in acid electrolyte is shown in the insets⁶⁵.

the drawbacks of perfluorosulphonic membranes, nanoceramic fillers have been included in the polymer electrolyte network. Stonehart, Watanabe and co-workers⁷⁹ have successfully reduced the humidification constraints in PEMFCs by the inclusion of small amounts of SiO_2 and Pt/TiO_2 (~ 7 nm) nanoparticles to retain the electrochemically produced water inside the membrane. Similarly modified membranes, containing nanocrystalline ceramic oxide filler, have been demonstrated⁸⁰ to operate up to 150 °C. Although it has been hypothesized^{75–77} that the inorganic filler induces structural changes in the polymer matrix, the water-retention mechanism appears more likely to be favoured by the presence of acidic functional groups on the surface of nanoparticle fillers⁸¹. At present, there are no indications that the transport properties are significantly affected by the filler⁸². However, the greater water retention capability of the composite membrane at high temperatures (130 °C–150 °C) and under low humidity⁸¹ should promote the ‘vehicular mechanism’ of proton conduction as occurs at lower temperatures⁸³. Investigation of the lifetime behaviour

of composite membranes, under low humidity, needs to be carried out in the next few years to assess these electrolyte materials.

Within the PEMFCs, the Pt/C catalyst is intimately mixed with the electrolyte ionomer to form a composite catalyst layer extending the three-phase reaction zone. This is similar to the composite cathode approach in lithium-ion batteries where the electrode consists of two interpenetrating networks for electron and ion conduction; the benefit of this approach is an enhancement of the interfacial region between catalyst particles and ionomer^{62,84}. A reduction in the Pt content to significantly less than 0.5 mg cm^{-2} without degrading the cell performance and life-time has been demonstrated^{62,84}. Following this general concept, durable multi-level MEAs are being developed (3M Corporation) using high-speed precision coating technologies and an automated assembly process⁸⁵. Part of the MEA is a nanostructured thin-film catalyst based on platinum-coated nano-whiskers. The approach uses highly oriented, high-aspect-ratio single-crystalline whiskers of an organic pigment material. Typically there are 3×10^9 to 5×10^9 whiskers cm^{-2} . This support permits suitable specific activity of the applied catalysts and aids processing and manufacturing. However, the electrocatalytic activities so obtained are comparable to catalyst-ionomer inks. Platinum-coated nano-whiskers and a cross-section of the MEA are shown in Fig. 8.

The trend towards nanomaterials is not limited to low-temperature fuel cells. Nanostructured electro-ceramic materials are increasingly used in intermediate-temperature solid oxide fuel cells (IT-SOFCs). Although one may start with nanosized particles in the fabrication of SOFCs materials, these are often modified by the temperatures required for cell fabrication ($>1,000$ °C), thus forming microstructured components with electro-catalytic and ion-conduction properties different from the typical polycrystalline materials⁸⁶. Nanosized YSZ ($8\% Y_2O_3-ZrO_2$) and ceria-based (CGO, SDC, YDC) powders permit a reduction of the firing temperature during the membrane-forming step in the cell fabrication procedure, because their sintering properties differ from those of polycrystalline powders⁸⁷. Furthermore, nanocrystalline ceria, which is characterized by mixed electronic-ionic conduction properties, promotes the charge transfer reactions at the electrode-electrolyte interface⁸⁷.

Ionic charge carriers in electro-ceramic materials originate from point defects. In nanostructured systems, the significantly larger area of interface and grain boundaries produces an increase in the density of mobile defects in the space-charge region. This in turn leads to a completely different electrochemical behaviour from that of bulk polycrystalline materials^{86,89}. According to Maier⁸⁸, these ‘trivial’ size effects, resulting simply from an increased proportion of the interface, should be distinguished from ‘true’ size effects occurring when the particle size is smaller than four times the Debye length, where the local properties are changed in terms of ionic and electronic charge-carrier transport. Interestingly, the same space-charge model was

used by Maier to explain the observed increase in ionic conductivity of dry or hybrid Li-based polymer systems loaded with nano-inorganic fillers (SiO_2 , Al_2O_3 , TiO_2) as discussed previously.

Notwithstanding the importance of nanostructured materials, the performance of practical fuel cells remains limited by scale-up, stack housing design, gas manifold and sealing. Although progress has been achieved in the direct electrochemical oxidation of alcohol and hydrocarbon fuels^{62,90,91}, fuel cells are still mostly fed by hydrogen. Much research is now focused on nanostructured hydrides including carbon nanotubes, nanomagnesium-based hydrides, metal-hydride/carbon nanocomposites, and alanates for hydrogen storage^{92,93}. Early reports suggested hydrogen adsorption capacities of 14–20 wt% for K- and Li-doped carbon nanotubes^{94,95}, but today's reliable hydrogen-storage capacities in single-walled carbon nanotubes appear comparable to or even less than those of metal hydrides^{96–98}, and probably not sufficient to store the amount of hydrogen required for automotive applications, which has been set by the US Department of Energy as 6.5% (ref. 98). Recent developments in this field include modification of Mg-hydrides with transition metals^{99,100}, and the investigation of boron-nitride nanostructures¹⁰¹. Magnesium hydride, MgH_2 , is often modified by high-energy ball-milling with alloying elements including⁹⁹ Ni, Cu, Ti, Nb and Al so as to obtain, after 20 h of milling, nanoparticles in the range of 20–30 nm providing hydrogen-storage capacities of about 6–11 wt% (refs 99, 100). Besides improving the hydrogen sorption kinetics of MgH_2 , partial substitution of Al for Mg in Mg_2Ni hydrogen storage systems seems to increase the life-cycle characteristics, as a consequence of the existence of an Al_2O_3 film on the alloy surface⁹⁹. Further advances resulted from the investigation of MgH_2 -V nanocomposites¹⁰⁰ and the addition of very small amounts of nanoparticulate transition metal oxides (Nb_2O_5 , WO_3 , Cr_2O_3) to Mg-based hydrides¹⁰². The presence of vanadium as well as the particular nanostructure of the nanocomposite aids the hydrogen penetration into the material. Also, in the case of transition metal oxide promoters, the catalytic effect of compounds such as Cr_2O_3 , the reactive mechanical grinding and the nanosized particles seem to produce a substantial improvement in the adsorption and desorption properties of magnesium¹⁰².

CONCLUSION

It is a regrettable feature of important scientific discoveries that they often suffer from hyperbole; perhaps it has always been so, but the speed of today's communications exacerbates the situation. Nanoscience suffers from this disease. Yet there are many genuine scientific advances that fall under the umbrella of nanoscience. This short review demonstrates how moving from bulk materials to the nanoscale can significantly change electrode and electrolyte properties, and consequently their performance in devices for energy storage and conversion. In some cases the effects may be simple

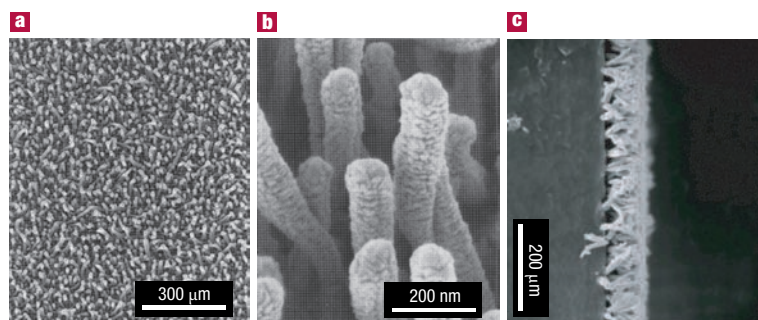


Figure 8 Platinum-coated nanostructured whisker supports (0.25 mg cm^{-2}). a, Plane view; b, 45° view (higher magnification). The nanostructured film of the MEA (c) shows the Pt-coated nanostructured whiskers sandwiched between the PEM and the gas-diffusion layer. Courtesy of R. Atanasoski, 3M, St. Paul, Minnesota, USA.

consequences of a reduction in size, for example when nanoparticulate electrodes or electrocatalysts lead to higher electrode/electrolyte contact areas and hence higher rates of electrode reaction. In others the effects may be more subtle, involving internally nanostructured materials or nanostructures with particular morphologies, for example the nanotubes. Space-charge effects at the interface between small particles can result in substantial improvements of properties. There is a profound effect of spatial confinement and contribution of surfaces, due to small particle size, on many of the properties of materials; this challenges us to develop new theory or at least adapt and develop theories that have been established for bulk materials. We also foresee that this subject will bring together the disciplines of materials chemistry and surface science, as both are necessary to understand nanomaterials.

doi:10.1038/nmat1368

References

- Nazar, L. F. *et al.* Nanostructured materials for energy storage. *Int. J. Inorg. Mater.* **3**, 191–200 (2001).
- Hirshes, M. Nanoscale materials for energy storage. *Mater. Sci. Eng. B* **108**, 1 (2004).
- Scrosati, B. Challenge of portable power. *Nature* **373**, 557–558 (1995).
- Tarascon, J.-M. & Armand, M. Issues and challenges facing rechargeable batteries. *Nature* **414**, 359–367 (2001).
- Wakihara, W. & Yamamoto, O. (eds) *Lithium Ion Batteries—Fundamentals and Performance* (Kodansha-Wiley-VCH, Weinheim, 1998).
- van Schalkwijk, W. & Scrosati, B. (eds) *Advances in Lithium-Ion Batteries* (Kluwer Academic/Plenum, New York, 2002).
- Huggins, R. A. in *Handbook of Battery Materials* (ed. Besenhard, J. O.) Part III, Chapter 4 (Wiley-VCH, Weinheim, 1999).
- Winter, M. & Besenhard, J. O. Electrochemical lithiation of tin and tin-based intermetallic and composites. *Electrochim. Acta* **45**, 31–50 (1999).
- Nazar, L. F. & Crosnier, O. In *Lithium Batteries Science and Technology* (eds Nazri, G.-A. & Pistoia, G.) 112–143 (Kluwer Academic/Plenum, Boston, 2004).
- Idota, Y., Kabuto, T., Matsufuji, A., Maekawa, Y. & Miyasaki, T. Tin-based amorphous oxides: a high-capacity lithium-ion storage material. *Science* **276**, 1395–1397 (1997).
- Mao, O. & Dahn, J. R. Mechanically alloyed Sn-Fe(-C) powders as anode materials for Li ion batteries. III. $\text{Sn}_3\text{Fe}:\text{SnFe}_3\text{C}$ active/inactive composites. *J. Electrochem. Soc.* **146**, 423–427 (1999).
- Beaulieu, L. Y. & Dahn, J. R. The reaction of lithium with Sn-Mn-C intermetallics prepared by mechanical alloying. *J. Electrochem. Soc.* **147**, 3237–3241 (2000).
- Graetz, J., Ahn, C. C., Yazami, R. & Fuetz, B. Highly reversible lithium storage in nanostructured silicon. *Electrochim. Solid-State Lett.* **6**, A194–197 (2003).
- Yang, J. *et al.* Si/C composites for high capacity lithium storage materials. *Electrochim. Solid-State Lett.* **6**, A154–156 (2003).
- Novak, P. *et al.* in *Int. Meeting Li Batteries IMLB12 Nara, Japan Abstract 9* (2004).
- Ikedo, H. *et al.* in *Proc. 42nd Battery Symposium, Yokohama, Japan* 282 (2001).
- Green, M., Fielder, E., Scrosati, B., Wachtler, M. & Serra Moreno, J. Structured silicon anodes for lithium battery applications. *Electrochim. Solid-State Lett.* **6**, A75–79 (2003).
- Armstrong, A. R., Armstrong, G., Canales, Garcia, J. R. & Bruce, P. G. Lithium intercalation into TiO_2 -B nanowires. *Adv. Mater.* (in the press).
- Poizot, P., Laruelle, S., Grugeon, S., Dupont, L. & Tarascon, J.-M. Nano-sized

- transition metal oxides as negative electrode material for lithium-ion batteries. *Nature* **407**, 496–499 (2000).
20. Tarascon, J.-M., Grubeon, S., Laruelle, S., Larcher, D. & Poizat, P. In *Lithium Batteries Science and Technology* (eds Nazri, G.-A. & Pistoia, G.) Ch. 7, 220–246 (Kluwer Academic/Plenum, Boston, 2004).
 21. Denis, S., Baudrin, E., Touboul, M. & Tarascon, J.-M. Synthesis and electrochemical properties vs. Li of amorphous vanadates of general formula RVO_3 ($R = \text{In, Cr, Fe, Al, Y}$) *J. Electrochem. Soc.* **144**, 4099–4109 (1997).
 22. Leroux, F., Coward, G. R., Power, W. P. & Nazar, L. F. Understanding the nature of low-potential Li uptake into high volumetric capacity molybdenum oxides. *Electrochem Solid-State Lett.* **1**, 255–258 (1998).
 23. Balaya, P., Li, H., Kienle, L. & Maier, J. Fully reversible homogeneous Li storage in RuO_2 with high capacity. *Adv. Funct. Mater.* **13**, 621–625 (2003).
 24. Badway, F., Cosandey, F., Pereira, N. & Amatucci, G. G. Carbon metal fluoride nanocomposites: high capacity reversible metal fluoride conversion materials as rechargeable positive electrodes for Li batteries. *J. Electrochem. Soc.* **150**, A1318–A1327 (2003).
 25. Li, H., Ritcher, G. & Maier, J. Reversible formation and decomposition of LiF clusters using transition metal fluorides as precursors and their application in rechargeable Li batteries. *Adv. Mater.* **15**, 736–739 (2003).
 26. Jammik, J. & Maier, J. Nanocrystallinity effects in lithium battery materials. Aspects of nano-ionics. Part IV. *Phys. Chem. Chem. Phys.* **5**, 5215–5220 (2003).
 27. Larcher, D. *et al.* Effect of particle size on lithium intercalation into $\alpha\text{-Fe}_2\text{O}_3$. *J. Electrochem. Soc.* **150**, A133–A139 (2003).
 28. Sides, C. R., Li, N. C., Patrissi, C. J., Scrosati, B. & Martin, C. R. Nanoscale materials for lithium-ion batteries. *Mater. Res. Bull.* **27**, 604–607 (2002).
 29. Nordlinder, S., Edström, K. & Gustafsson, T. Electrochemistry of vanadium oxide nanotubes. *Electrochem. Solid State Lett.* **4**, A129 (2001).
 30. Le, D. B. *et al.* High surface area V_2O_5 aerogel intercalation electrodes. *J. Electrochem. Soc.* **143**, 2099–2104 (1996).
 31. Dong, W., Rolison, D. R. & Dunn, B. Electrochemical properties of high surface area vanadium oxides aerogels. *Electrochem. Solid State Lett.* **3**, 457–459 (2000).
 32. Thackeray, M. M., David, W. I. F., Bruce, P. G. & Goodenough, J. B. Lithium insertion into manganese spinels. *Mater. Res. Bull.* **18**, 461–472 (1983).
 33. Robertson, A. D., Armstrong, A. R. & Bruce, P. G. Layered $\text{Li}_x\text{Mn}_2\text{Co}_{1-x}\text{O}_2$ intercalation electrodes: influence of ion exchange on capacity and structure upon cycling. *Chem. Mater.* **13**, 2380–2386 (2001).
 34. Shao-Horn, Y. *et al.* Structural characterisation of layered LiMnO_2 electrodes by electron diffraction and lattice imaging. *J. Electrochem. Soc.* **146**, 2404–2412 (1999).
 35. Wang, H. F., Jang, Y. I. & Chiang, Y.-M. Origin of cycling stability in monoclinic and orthorhombic-phase lithium manganese oxide cathodes. *Electrochem. Solid-State Lett.* **2**, 490–493 (1999).
 36. Kang, S. H., Goodenough, J. B. & Rabenberg, L. K. Effect of ball-milling on 3 V capacity of lithium manganese oxospinel cathodes. *Chem. Mater.* **13**, 1758–1764 (2001).
 37. Reed, J., Ceder, G. & van der Ven, A. Layered-to-spinel phase transformation in Li_xMnO_2 . *Electrochem. Solid-State Lett.* **4**, A78–81 (2001).
 38. Padhi, A. K., Nanjundaswamy, K. S., Masquelier, C., Okada, S. & Goodenough, J. B. Effect of structure on the $\text{Fe}^{3+}/\text{Fe}^{2+}$ redox couple in iron phosphates. *J. Electrochem. Soc.* **144**, 1609–1613 (1997).
 39. Ravet, A. *et al.* Electroactivity of natural and synthetic triphylite. *J. Power Sources* **97–98**, 503–507 (2001).
 40. Huang, H., Yin, S.-C. & Nazar, L. F. Approaching theoretical capacity of LiFePO_4 at room temperature and high rates. *Electrochem. Solid-State Lett.* **4**, A170–A172 (2001).
 41. Croce, F., Scrosati, B., Sides, B. R. & Martin, C. R. in *206th Meeting Electrochemical Society, Honolulu, Hawaii* Abstract 241 (2004).
 42. Scrosati, B. & Vincent, C. A. Polymer electrolytes: the key to lithium polymer batteries. *Mater. Res. Soc. Bull.* **25**, 28–30 (2000).
 43. Croce, F., Appetecchi, G. B., Persi, L. & Scrosati, B. Nanocomposite polymer electrolytes for lithium batteries. *Nature* **394**, 456–458 (1998).
 44. MacFarlane, D. R., Newman, P. J., Nairn, K. M. & Forsyth, M. Lithium-ion conducting ceramic/polyether composites. *Electrochim. Acta* **43**, 1333–1337 (1998).
 45. Kumar, B., Rodrigues, S. J. & Scanlon, L. Ionic conductivity of polymer–ceramic composites. *J. Electrochem. Soc.* **148**, A1191–A1195 (2001).
 46. Maier, J. Ionic conduction in space charge regions. *Prog. Solid State Chem.* **23**, 171–263 (1995).
 47. Appetecchi, G. B., Croce, F., Persi, L., Ronci, F. & Scrosati, B. Transport and interfacial properties of composite polymer electrolytes. *Electrochim. Acta* **45**, 1481–1490 (2000).
 48. Angell, C. A., Liu, C. & Sanchez, S. Rubbery solid electrolytes with dominant cationic transport and high ambient conductivity. *Nature* **362**, 137–139 (1993).
 49. Hawett, P. C., MacFarlane, D. R. & Hollenkamp, A. F. High lithium metal cycling efficiency in a room-temperature ionic liquid. *Electrochem. Solid-State Lett.* **7**, A97–A101 (2004).
 50. MacGlashan, G., Andreev, Y. G. & Bruce, P. G. The structure of poly(ethylene oxide) $_x\text{LiAsF}_6$. *Nature* **398**, 792–794 (1999).
 51. Gadjouroua, Z., Andreev, Y. G., Tunstall D. P. & Bruce, P. G. Ionic conductivity in crystalline polymer electrolytes. *Nature* **412**, 520–523 (2001).
 52. Stoeva, Z., Martin-Litas, I., Staunton, E., Andreev, Y. G. & Bruce, P. G. Ionic conductivity in the crystalline polymer electrolytes $\text{PEO}_x\text{:LiXF}_6$, $X = \text{P, As, Sb}$. *J. Am. Chem. Soc.* **125**, 4619–4626 (2003).
 53. Christie, A. M., Lilley, S. J., Staunton, E., Andreev, Y. G. & Bruce, P. G. Increasing the conductivity of crystalline polymer electrolytes. *Nature* **433**, 50–53 (2005).
 54. Conway, B. E. *Electrochemical Supercapacitors*. (Kluwer Academic/Plenum, New York, 1999).
 55. Mastragostino, M., Arbizzani, C. & Soavi, F. In *Advances in Lithium-Ion Batteries*. (Van Schalkwijk, W. & Scrosati, B., eds) Ch. 16, 481–505 (Kluwer Academic/Plenum, New York, 2002).
 56. Arbizzani, C., Mastragostino, M. & Soavi, S. New trends in electrochemical supercapacitors. *J. Power Sources* **100**, 164–170 (2001).
 57. Wang, J. *et al.* Morphological effects on the electrical and electrochemical properties of carbon aerogels. *J. Electrochem. Soc.* **148**, D75–77 (2001).
 58. Niu, C., Sichjel, E. K., Hoch, R., Hoi, D. & Tennent, H. High power electrochemical capacitors based on carbon nanotube electrodes. *Appl. Phys. Lett.* **70**, 1480–1482 (1997).
 59. Nelson, P. A. & Owen, J. R. A high-performance supercapacitor/battery hybrid incorporating templated mesoporous electrodes. *J. Electrochem. Soc.* **150**, A1313–A1317 (2003).
 60. Amatucci, G. G., Badway, F., Du Pasquier, A. & Zheng, T. An asymmetric hybrid nonaqueous energy storage cell. *J. Electrochem. Soc.* **148**, A930–A939 (2001).
 61. Brodd, R. J. *et al.* Batteries 1977 to 2002. *J. Electrochem. Soc.* **151**, K1–K11 (2004).
 62. Srinivasan, S., Mosdale, R., Stevens, P. & Yang, C. Fuel cells: reaching the era of clean and efficient power generation in the twenty-first century. *Annu. Rev. Energy Environ.* **24**, 281–238 (1999).
 63. Giordano, N. *et al.* Analysis of platinum particle size and oxygen reduction in phosphoric acid. *Electrochim. Acta* **36**, 1979–1984 (1991).
 64. Freund, A., Lang, J., Lehman, T. & Starz, K. A. Improved Pt alloy catalysts for fuel cells. *Catal. Today* **27**, 279–283 (1996).
 65. Mukerjee, S., Srinivasan, S., Soriaga, M. P. & McBreen, J. Role of structural and electronic properties of Pt and Pt alloys on electrocatalysis of oxygen reduction. An *in-situ* XANES and EXAFS investigation. *J. Electrochem. Soc.* **142**, 1409–1422 (1995).
 66. Aricò, A. S., Srinivasan, S. & Antonucci, V. DMFCs: From fundamental aspects to technology development. *Fuel Cells* **1**, 133–161 (2001).
 67. Schmidt, T. J. *et al.* Electrochemical activity of Pt–Ru alloy colloids for CO and CO/H_2 electrooxidation: stripping voltammetry and rotating-disk measurements. *Langmuir* **14**, 2591–2595 (1997).
 68. Chrzanowski, W. & Wieckowski, A. Enhancement in methanol oxidation by spontaneously deposited ruthenium on low-index platinum-electrodes. *Catal. Lett.* **50**, 69–75 (1998).
 69. Brankovic, S. R., Wang, J. X. & Adzic, R. R. Pt submonolayers on Ru nanoparticles—a novel low Pt loading, high CO tolerance fuel-cell electrocatalyst. *Electrochem. Solid-State Lett.* **4**, A217–A220 (2001).
 70. Hockaday, R. G. *et al.* in *Proc. Fuel Cell Seminar, Portland, Oregon, USA* 791–794 (Courtesy Associates, Washington DC, 2000).
 71. Sun, G. R., Wang, J. T. & Savinell, R. F. Iron(III) tetramethoxyphenylporphyrin (Fetmpp) as methanol tolerant electrocatalyst for oxygen reduction in direct methanol fuel-cells. *J. Appl. Electrochem.* **28**, 1087–1093 (1998).
 72. Reeve, R. W., Christensen, P. A., Hammett, A., Haydock, S. A. & Roy, S. C. Methanol tolerant oxygen reduction catalysts based on transition metal sulfides. *J. Electrochem. Soc.* **145**, 3463–3471 (1998).
 73. Nolte, R., Ledjeff, K., Bauer, M. & Mulhaupt, R. Partially sulfonated poly(arylene ether sulfone)—a versatile proton conducting membrane material for modern energy conversion technologies. *J. Membrane Sci.* **83**, 211–220 (1993).
 74. Kerres, J., Ullrich, A., Meier, F. & Haring, T. Synthesis and characterization of novel acid-base polymer blends for application in membrane fuel cells. *Solid State Ionics* **125**, 243–249 (1999).
 75. Alberti, G. & Casciola, M. Composite membranes for medium-temperature PEM fuel cells. *Annu. Rev. Mater. Res.* **33**, 129–154 (2003).
 76. Savadogo, O. Emerging membranes for electrochemical systems: (I) solid polymer electrolyte membranes for fuel cell systems. *J. New Mater. Electrochem. Syst.* **1**, 47–66 (1998).
 77. Li, Q., He, R., Jensen, J. O. & Bjerrum, N. J. Approaches and recent development of polymer electrolyte membranes for fuel cells operating above 100 °C. *Chem. Mater.* **15**, 4896–4815 (2003).
 78. Kreuer, K. D. On the development of proton conducting polymer membranes for hydrogen and methanol fuel cells. *J. Membrane Sci.* **185**, 29–39 (2001).
 79. Watanabe, M., Uchida, H., Seki, Y., Emori, M. & Stonehart, P. Self-humidifying polymer electrolyte membranes for fuel cells. *J. Electrochem. Soc.* **143**, 3847–3852 (1996).
 80. Aricò, A. S., Creti, P., Antonucci, P. L. & Antonucci, V. Comparison of ethanol and methanol oxidation in a liquid feed solid polymer electrolyte fuel cells at high temperature. *Electrochem. Solid-State Lett.* **1**, 66–68 (1998).
 81. Aricò, A. S., Baglio, V., Di Blasi, A. & Antonucci, V. FTIR spectroscopic investigation of inorganic fillers for composite DMFC membranes. *Electrochem. Commun.* **5**, 862–866 (2003).
 82. Kreuer, K. D., Paddison, S. J., Spohr, E. & Schuster, M. Transport in proton conductors for fuel cell applications: simulation, elementary reactions and phenomenology. **104**, 4637–4678 (2004).

83. Kreuer, K. D. On the development of proton conducting materials for technological applications. *Solid State Ionics* **97**, 1–15 (1997).
84. Debe, M. K. *Handbook of Fuel Cells—Fundamentals, Technology and Applications* Vol. 3 (eds Vielstich, W., Gasteiger, H. A. & Lamm, A.) Ch. 45, 576–589 (Wiley, Chichester, UK, 2003).
85. Atanasoski, R. in *4th Int. Conf. Applications of Conducting Polymers, ICCP-4, Como, Italy Abstract 22* (2004).
86. Schoonman, J. Nanoionics. *Solid State Ionics* **157**, 319–326 (2003).
87. Steele, B. C. H. Current status of intermediate temperature fuel cells (It-SOFCs). *European Fuel Cell News* **7**, 16–19 (2000).
88. Maier, J. Defect chemistry and ion transport in nanostructured materials. Part II Aspects of nanoionics. *Solid State Ionics* **157**, 327–334 (2003).
89. Knauth, P & Tuller, H. L. Solid-state ionics: roots, status, and future-prospects. *J. Am. Ceram. Soc.* **85**, 1654–1680 (2002).
90. Perry Murray, E., Tsai, T. & Barnett, S. A. A direct-methane fuel cell with a ceria-based anode. *Nature* **400**, 649–651 (1999).
91. Park, S., Vohs, J. M. & Gorte, R. J. Direct oxidation of hydrocarbons in a solid-oxide fuel cell. *Nature* **404**, 265–267 (2000).
92. Zhou, Y. P., Feng, K., Sun, Y. & Zhou, L. A brief review on the study of hydrogen storage in terms of carbon nanotubes. *Prog. Chem.* **15**, 345–350 (2003).
93. Schlappach, L. & Zuttel, A. Hydrogen-storage materials for mobile applications. *Nature* **414**, 353–358 (2001).
94. Dillon, A. C. *et al.* Storage of hydrogen in single-walled carbon nanotubes. *Nature* **386**, 377–379 (1997).
95. Chambers, A., Park, C., Baker, R. T. K. & Rodriguez, N. M. Hydrogen storage in graphite nanofibers. *J. Phys. Chem.* **102**, 4253–4256 (1998).
96. Yang, R. T. Hydrogen storage by alkali-doped carbon nanotubes—revisited. *Carbon* **38**, 623–626 (2000).
97. Dillon, A. C. & Heben, M. J. Hydrogen Storage using carbon adsorbents—past, present and future. *Appl. Phys. A* **72**, 133–142 (2001).
98. Hirscher, M. & Becher, M. Hydrogen storage in carbon nanotubes. *J. Nanosci. Nanotechnol.* **3**, 3–17 (2003).
99. Shang, C. X., Bououdina, M., Song, Y. & Guo, Z. X. Mechanical alloying and electronic simulation of MgH₂-M systems (M=Al, Ti, Fe, Ni, Cu, and Nb) for hydrogen storage. *Int. J. Hydrogen Energy* **29**, 73–80 (2004).
100. Bobet, J. L., Grigorova, E., Khrussanova, M., Khristov, M. & Peshev, P. Hydrogen sorption properties of the nanocomposite 90wt.% Mg₂Ni–10 wt.% V. *J. Alloys Compounds* **356**, 593–597 (2003).
101. Ma, R. Z. *et al.* Synthesis of boron-nitride nanofibers and measurement of their hydrogen uptake capacity. *Appl. Phys. Lett.* **81**, 5225–5227 (2002).
102. Bobet, J. L., Desmoulinckiewicz, S., Grigorova, E., Cansell, F. & Chevalier, B. Addition of nanosized Cr₂O₃ to magnesium for improvement of the hydrogen sorption properties. *J. Alloys Compounds* **351**, 217–221 (2003).
103. Audemer, A., Wurm, C., Morcrette, M., Gwizdala, S. & Masquellier, C. Carbon-coated metal bearing powders and process for production thereof. World Patent WO 04/001881 A2 (2004).

Acknowledgements

We thank M. Mastragostino of the university of Bologna for suggestions and help in completing the supercapacitors part of this review. Support from the European Network of Excellence 'ALISTORE' network is acknowledged. P.G.B. is indebted to the Royal Society for financial support. Correspondence should be addressed to B.S.

Competing financial interests

The authors declare that they have no competing financial interests.

Nanoionics: ion transport and electrochemical storage in confined systems

The past two decades have shown that the exploration of properties on the nanoscale can lead to substantially new insights regarding fundamental issues, but also to novel technological perspectives. Simultaneously it became so fashionable to decorate activities with the prefix 'nano' that it has become devalued through overuse. Regardless of fashion and prejudice, this article shows that the crystallizing field of 'nanoionics' bears the conceptual and technological potential that justifies comparison with the well-acknowledged area of nanoelectronics. Demonstrating this potential implies both emphasizing the indispensability of electrochemical devices that rely on ion transport and complement the world of electronics, and working out the drastic impact of interfaces and size effects on mass transfer, transport and storage. The benefits for technology are expected to lie essentially in the field of room-temperature devices, and in particular in artificial self-sustaining structures to which both nanoelectronics and nanoionics might contribute synergistically.

J. MAIER

is in the Max-Planck-Institut für Festkörperforschung, 70569 Stuttgart, Germany.
e-mail: s.weiglein@fkf.mpg.de

The triumph of electronics in both science and daily life relies, on the one hand, on the availability of solid materials in which atomic constituents exhibit negligible mobilities whereas electronic carriers can be easily excited and transferred; and, on the other, on the necessity of fast and precise information exchange. However, electronic devices cannot satisfy all the technological needs of our society: as far as the transformation of chemical to electrical energy or the chemical storage of electrical energy is concerned — as is possible in batteries and fuel cells, or as far as the transformation of chemical in electrical information is concerned — as verified in (electro)chemical sensors, electrochemical devices are indispensable^{1–4}. Solid electrochemical devices use the fact that (at least) one ionic component is immobile whereas another ionic component is highly mobile, and hence combine mechanical durability and electrochemical functionality. Such solids may be solid electrolytes — that is, pure ion-conducting solids — but they may also be mixed conducting solids that exhibit both significant electronic and ionic conductivities and can, for example, be used as powerful electrodes. Mixed conductors can also be used as key materials in related devices such as chemical sensors, chemical

filters, chemical reactors and electrochromic windows. Figure 1 provides a schematic overview by using the example of oxide ion conductivity. Beyond that, the study of mixed conductors offers a general phenomenological approach to electrically relevant solids in which the pure ionic and the pure electronic conductor appear as special cases.

In the nanometre regime, interfaces are so closely spaced that their influence on the overall property can become significant if not prevailing. It can even no longer be taken for granted that one can assume semi-infinite boundary conditions; in other words, it cannot be taken for granted that, with increasing distance, the impact of the interface dies off to the bulk value, because the next interface might already be perceptible. In interfacially controlled materials the overall impact of the interfacial regions increases with decreasing size. As long as their local influence is identical or comparable with that of isolated interfaces we may use the term 'trivial size effects', whereas the term 'true size effects' implies that interfaces perceive each other^{5–8}. As long as we can ignore the effect of curvature this distinction is possible.

Nanoelectronics^{9–12} is essentially based on the quantum-mechanical confinement effect, a true size effect as a consequence of which the energy of delocalized electrons increases with decreasing size. As far as electronic devices¹³ are concerned, trivial size effects are important in varistors (insulating grain boundaries become conductive under bias), PCT ceramics (resistance shows a